This is to certify that the
thesis entitled

PYROPHOSPHATE AS A DYNAMIC PROBE OF THE HUMAN RNA POLYMERASE II MECHANISM

presented by

Woo Jung Moon

has been accepted towards fulfillment
of the requirements for the

M.S. degree in Biochemistry and Molecular Biology

Major Professor's Signature

4/29/08

Date

PYROPHOSPHATE AS A DYNAMIC PROBE OF THE HUMAN RNA POLYMERASE II MECHANISM

By

Woo Jung Moon

A THESIS

Submitted to
Michigan State University
in partial fulfillment of the requirements
for the degree of

MASTER OF SCIENCE

Department of Biochemistry and Molecular Biology

2008

ABSTRACT

PYROPHOSPHATE AS A DYNAMIC PROBE OF THE HUMAN RNA POLYMERASE II MECHANISM

By

Woo Jung Moon

Pyrophosphate, a product released after phosphodiester bond synthesis, can in large quantities catalyze a reverse RNA synthesis reaction called pyrophosphorolysis. In this reaction, pyrophosphate removes the 3'-NMP (nucleoside monophosphate) from a nascent RNA chain to release nucleoside triphosphate (NTP). This thesis will describe four important aspects of human RNA polymerase II mechanism learned through experiments utilizing pyrophosphate as a dynamic probe. First, although mononucleotide products are expected from pyrophosphorolysis, we find that exposing human RNA polymerase II elongation complex to pyrophosphate can result in apparent cleavage of dinucleotide that looks and behaves similarly to dinucleotide cleavage products from TFIIS. Second, in addition to catalyzing dinucleotide cleavage reactions, pyrophosphate can suppress transcriptional pausing, presumably by retaining the elongation complex on the active synthesis pathway. Third, pyrophosphate is observed to be fairly important in maintaining fidelity during elongation as it suppresses incorporation of incorrect substrate NTP. Fourth, we find that utilizing pyrophosphate slows down elongation enough to observe the internal mechanism of the polymerase. It appears that pre- and post-translocated elongation complex are present together and we argue that translocation appears to progress via a thermal ratchet.

I dedicate this work to my wife Erica and family who supported me throughout the years

ACKNOWLDGEMENT

I would like to thank Dr. McCormick, Dr. Maher and Mrs Bethany Heinlen for guiding me through the past five years. Though there have been ups and downs, they made the ride as smooth as possible for me. I also extend my thanks to the College of Osteopathic Medicine at Michigan State University for the continued support for medical students pursuing research.

My committee members Drs David Arnosti and Hanggao Yan have been wonderful as they helped me in difficult times and made my transition from classroom to research much easier.

My thanks also go to Dr. Maria Zavodszky for being a second mentor for me. She has been a great resource throughout the years and has given me great advice in terms of science and life.

I would also like to thank all my family members as they supported me through good and bad. My wife Erica has been the most supportive family member as she has helped me achieve things that I couldn't have done without her. I would not be receiving this degree without her support and encouragement.

The Burton laboratory has been a wonderful place for me as well. Drs Xueqian Gong, Chunfen Zhang and Yalin Xiong have been like a family to me. I also extend my thanks to all lab members, Rita Grantner, Anthony Nazioni and Jenna Doe who have made many things possible for me.

Last but not least, I would like to thank my advisor Dr. Zach Burton for giving me the opportunity to work in his lab and giving me valuable advice. It has been a wonderful ride.

TABLE OF CONTENTS

List of Figures vi

List of Abbreviations vii

Chapter 1
Introduction 1
Prokaryotic RNA polymerase structure 2
Eukaryotic RNA polymerase II structure 6
Eukaryotic transcription elongation factor TFIIF 9
Eukaryotic transcription elongation factor TFIIS 10
Pyrophosphate and the mechanism of multi-subunit RNA polymerase 17
The elongation mechanism of multi-subunit RNA polymerases 19
NTP-driven translocation and main enzyme channel loading ... 19
Secondary pore NTP loading models: Power stroke or brownian ratchet? 23
References 29

Chapter 2
Pyrophosphate as a dynamic probe of the human RNA polymerase II mechanism 37
Summary 37
Introduction 38
Experimental procedures 41
Cell culture, extracts and proteins 41
Pyrophosphorolysis 41
Elongation reactions 43
Misincorporation studies 44
Analog studies 45
Results 45
PPi stimulates 3'-dinucleotide cleavage of a nascent RNA 45
Effects of TFIIF and PPi on elongation and pausing 50
Effects of PPi on misincorporation and NTP scavenging 60
Effects of TFIIS 65
PPi inhibition of transcription at moderate NTP concentrations 74
Effects of PPi and NTPs on RNAP II burst kinetics 86
Discussion 89
NTP-assisted translocation 89
Thermal ratchet and NTP-assisted translocation 91
Suppression of pausing and TFIIS 92
References 95

LIST OF FIGURES

Figure 1.1 Similarities between prokaryotic and eukaryotic RNA polymerase 3

Figure 1.2 Binding of TFIIS to RNA polymerase II 11

Figure 1.3 Proposed active site mechanisms 14

Figure 1.4 Two NTP loading mechanisms 21

Figure 1.5 RNA polymerase active site dynamics 26

Figure 2.1 PPi induces cleavage of a dinucleotide 47

Figure 2.2 TFIIF and PPi suppress transcriptional pausing. TFIIF stimulates and pyrophosphate suppresses misincorporation 51

Figure 2.3 PPi inhibits elongation strongly at low NTP concentrations but not at high NTP concentrations 57

Figure 2.4 PPi suppresses incorporation of incorrect NTPs 61

Figure 2.5 When added prior to TFIIS, PPi appears to inhibit TFIIS-mediated A43→A41 dinucleotide cleavage 66

Figure 2.6 When added together, PPi does not inhibit TFIIS-mediated dinucleotide cleavage 70

Figure 2.7 PPi strongly inhibits elongation at moderate NTP concentrations 75

Figure 2.8 C46 elongation to C47 and C47 pyrophosphorolysis to C46 appear to be at dynamic equilibrium, indicating a mixture of pre- and post-translocated elongation complexes at the C47 stall position 82

Figure 2.9 PPi attenuates the amplitude of the burst in G44 synthesis at 100 μM but not at 2.5 mM GTP 88

Images in this thesis are included in color.

KEY TO ABBREVIATIONS

Mg^{2+}	Magnesium
DNAP	DNA polymerase
RNAP	RNA polymerase
RNA	Ribonucleic acid
DNA	Deoxyribonucleic acid
mRNA	Messenger RNA
snRNA	Small nuclear RNA
NTP	Nucleoside triphosphate
NMP	Nucleoside monophosphate
PPi	Pyrophosphate
S_N2	Bimolecular nucleophilic substitution
EDTA	Ethylenediaminetetraacetic acid
μM	Micromolar
mM	Millimolar
Tt	*Thermus thermophilus*
Sc	*Saccharomyces cerevisiae*
Hs	*Homo sapiens*

Chapter 1

Introduction

Eukaryotic RNA polymerase (RNAP) II is an essential enzyme that converts information stored in DNA to RNA in the form of pre-messenger RNA (pre-mRNA), micro RNAs and some small nuclear RNAs (snRNA) through a process called transcription (Conaway and Conaway, 1999; Nikolov and Burley, 1997; Shilatifard, 1998a, b). Processed messenger RNAs (mRNA) can be used as codes for protein synthesis. In contrast to eukaryotic systems that utilize three nuclear RNAPs for RNA synthesis, one RNAP synthesizes all RNA in prokaryotes and the enzyme is required for its survival (Vassylyev et al., 2002). For this reason, many antibiotics that have little or no impact on eukaryotic RNAP have been created to target bacterial RNAPs (Artsimovitch and Vassylyev, 2006; Villain-Guillot et al., 2007). Currently, the structure of human RNAP II remains unsolved. However, because yeast RNAP II is known to maintain 53% identity with human RNAP II (Cramer et al., 2001), it is commonly referred to when describing the mechanism and function of human RNAP II. Together, 12 eukaryotic RNA polymerase II subunits (Rpb1-12) comprise the core enzyme, but a functional polymerase can be obtained lacking Rpb4 and Rpb7, also known as the 10 subunit catalytic core (Cramer, 2004; Edwards et al., 1991). While Rpb4/7 heterodimer can dissociate from the core enzyme, and does not affect transcription elongation, Rpb4/7 plays important roles in promoter-dependent initiation (Choder, 2004; Edwards et al., 1991). A current understanding of the multi-subunit RNAP elongation mechanism is reviewed below. While important

factors such as transcription factor IIF (TFIIF), TFIIS and Pyrophosphate (PPi) and their effects will be the main focus of this thesis, recently solved crystal structures will be discussed that have revised our understanding of transcription elongation mechanisms dramatically. As seen in Figure 1.1, eukaryotic RNAP II and prokaryotic RNAP have conserved secondary, subunit and tertiary structures. For this reason, most believe that multi-subunit RNAPs utilize the same overall mechanism during transcription elongation (Landick, 2001; Vassylyev et al., 2002; von Hippel, 1998).

Prokaryotic RNA polymerase structure

Recently solved structures have given us insight into how multi-subunit RNAPs may operate during transcription elongation (Cramer et al., 2001; Gnatt et al., 2001; Vassylyev et al., 2002; Vassylyev et al., 2007a; Vassylyev et al., 2007b; Wang et al., 2006; Westover et al., 2004a, b). This section will describe the structure of *Thermus thermophilus* RNAP. Bacterial RNAP is composed of two α subunits (α2), β, β' and ω (collectively called the core enzyme) as well as a σ factor that can associate and dissociate during transcription (Figure 1.1A). Core RNAP together with σ factor is referred to as RNAP holoenzyme (Vassylyev et al., 2002). It is understood that σ factor dissociates during the transition from initiation to elongation because of steric hinderance between exiting nascent RNA and the σ_{3-4} linker (Mooney et al., 2005).

Figure 1.1 **Similarities between prokaryotic and eukaryotic RNA polymerase.** Different colors represent corresponding subunits between prokaryotic and eukaryotic polymerase. Green: β' and Rpb1, red: β and Rpb2, yellow: α and Rpb3, blue: α and Rpb11, orange: ω and Rpb6 in bacteria and yeast respectively. A) *Thermus thermophilus* RNA polymerase structure (PDB code: 2A6E). B) *Saccharomyces cerevisiae* RNA polymerase II structure (PDB code: 1I50). Subunits colored in gray are ones that do not have corresponding subunits in bacteria. Crystal structures were downloaded from www.pdb.org and were modified utilizing the PyMol molecular graphics system (www.pymol.org) by DeLano, W.L.

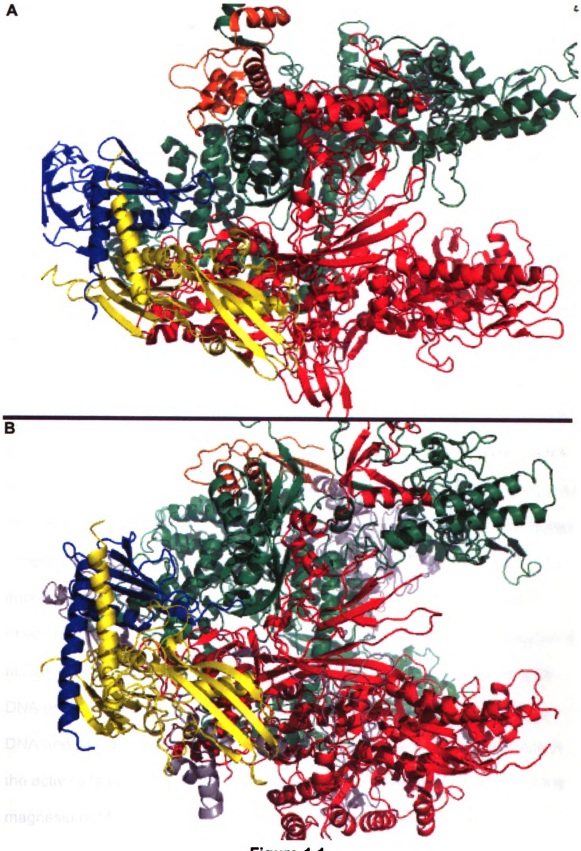

Figure 1.1

Two α subunits of bacterial RNAP are homologous to Rpb3 and Rpb11 in eukaryotic RNAP II while β' and β are similar to the two largest subunits in eukaryotic RNAP II, Rpb1 and Rpb2 respectively. Last but not least, ω corresponds to Rpb6 (Coulombe and Burton, 1999; Ebright, 2000; Sweetser et al., 1987). Although eukaryotic and prokaryotic RNAPs are not highly conserved in sequence, they are, however, evolutionarily conserved in their secondary structures (Figure 1.1). Multi-subunit RNAPs, therefore, are thought to behave similarly (Ebright, 2000; Landick, 2001; Steitz, 1998). The two largest subunits β and β' make up a crab claw-like pincer that maintains the main enzyme channel for DNA binding. Studies through simple elastic network modeling revealed that the two pincers are the most mobile elements of multi-subunit RNAPs (Van Wynsberghe et al., 2004). Clamping motions of the pincer may be an important feature of RNAP as open pincers can allow the enzyme to scan through a DNA template for a promoter, while a closed pincer may be important for holding onto the DNA substrate during elongation (Van Wynsberghe et al., 2004). The bridge α-helix, a structure conserved throughout evolution, is thought to play an important role in translocation as bent and straight orientations have been observed from different polymerase structures (Cramer et al., 2001; Vassylyev et al., 2002). Bending and straightening of the bridge helix may help translocate DNA one base at a time (Landick, 2004). Prokaryotic RNAP, similar to many DNA and single subunit RNAPs, is thought to utilize a two metal mechanism in the active site during RNA synthesis (Steitz, 1998; Wang et al., 2006). The first magnesium (Mg-I) is held together by three invariant aspartate acid resides

within the active site, while the second magnesium (Mg-II) is brought into the active site bound to the triphosphate tail of the incoming NTP (Westover et al., 2004a). Two Mg^{2+} in the active site help coordinate and distribute charge as the 3'-OH of the nascent RNA attacks the α-phosphate of incoming NTP in a S_N2 fashion reaction (Figure 1.3A) (Vassylyev et al., 2002; Vassylyev et al., 2007b). Current understanding of the detailed elongation mechanism will be discussed below together with trigger loop motions as recently solved crystal structures of bacterial and yeast transcription elongation complexes suggest trigger loop involvement in the chemical step of bond synthesis (Vassylyev et al., 2007b; Wang et al., 2006).

Eukaryotic RNA polymerase II structure

Structures of *Saccharomyces cerevisiae* RNAP II have commonly been referred to while describing the mechanism of all eukaryotic RNAP II. A 2.8 Å crystal structure solved in 2001 by the Kornberg lab has set the standard for all future eukaryotic RNAP II structures and has given us tremendous insight into how this complex enzyme may behave (Cramer et al., 2001). Since 2001, the Kornberg and Cramer labs have solved numerous yeast RNAP II structures at high resolution that allowed us to understand the mechanism in detail. Unlike prokaryotic RNAP described above, yeast RNAP II has 12 subunits, five of which correspond to specific homologous subunits in bacteria (Coulombe and Burton, 1999).

Yeast RNAP II retains structural similarities to the bacterial RNAP. First, as shown in Figure 1.1B, the crab claw-like pincer region, composed of Rpb1 and Rpb2, looks similar to its prokaryotic counterpart composed of homologous β' and β subunits. Rpb1 and Rpb2, the two most important subunits of the enzyme for catalysis are also highly mobile. DNA is thought to enter the enzyme by first contacting the jaw domain (Upper: Rpb1, Rpb9, Lower: Rpb5), followed by binding to and entering a highly positively charged main enzyme channel (or cleft). Because of its positive charge, main enzyme channel of multi-subunit RNAP is attractive to negatively charged objects, such as DNA. After recognizing the promotor, the clamp region of RNAP II (composed of Rpb1 and a small part of Rpb2) may close down on the DNA template strand (maximum of 30 Å movement), which may help improve transcription efficiency (Cramer et al., 2001; Gnatt et al., 2001; Landick, 2001). Another highly mobile region of RNAP II is an α-helix above the active site, known as the bridge helix. Structures of yeast RNAP II showed a straight bridge helix while some bacterial structure showed a bent bridge helix. Because of this finding, multi-subunit RNAP bridge helix is thought to be involved in translocation of the DNA/RNA hybrid (Cramer et al., 2001; Vassylyev et al., 2002; Zhang et al., 1999). Consistent with this idea, α-amanitin, a potent translocation inhibitor of eukaryotic RNAP II, which inhibits the translocation step of RNA synthesis (Bushnell et al., 2002; Chafin et al., 1995; Gong et al., 2004), binds tightly inside the secondary pore to the bridge helix (Bushnell et al., 2002). With α-amanitin bound to the bridge helix, RNAP II cannot

undergo conformation changes, resulting in an elongation complex that is unable to translocate.

Similar to the bacterial model, the eukaryotic RNAP II also has a funnel domain composed of four α-helices of the largest subunit. The funnel domain is a large portion of the secondary pore, a narrow tunnel that is thought to be the main entry way of NTPs and the route of PPi release by many scientists (Cramer et al., 2001; Gnatt et al., 2001; Westover et al., 2004a). The secondary pore is also where TFIIS enters the active site during elongation (Kettenberger et al., 2003, 2004). Details of the secondary pore substrate loading will be discussed below. Identical to bacterial RNAP, eukaryotic RNAP II also utilizes a two metal mechanism for bond synthesis. First Mg^{2+} (Mg-A) is held together by three invariant aspartic acid residues D481, D483, D485 within the active site (Cramer et al., 2001; Gnatt et al., 2001; Wang et al., 2006). A second Mg^{2+} (Mg-B), which is thought to enter the active site bound to the triphosphate tail of substrate NTP is held together in the active site by D481, D483 of Rpb1 as well as D837 of Rpb2 (Westover et al., 2004a). Again, metal ions distribute charges to improve S_N2 attack on the substrate NTP (i+1 NTP) α-phosphate by the 3'-OH of the RNA (Wang et al., 2006). The trigger loop is located near the bridge helix and is also thought to be involved in phosphodiester bond synthesis in a similar fashion to prokaryotes. Solved structures of the yeast RNAP II elongation complex suggest that DNA, after entering the cleft region, makes a 90° bend above the bridge helix before exiting the enzyme. Transcribed RNA separates from the template DNA

after 8-9nt synthesis and exits through the RNA exit channel on the enzyme surface (Gnatt et al., 2001).

Eukaryotic elongation factor TFIIF

Transcription factor IIF is a heterodimeric general elongation factor composed of RAP74 and RAP30 subunits and is important for accurate transcription initiation as well as elongation (Gaiser et al., 2000; Lei et al., 1998; Ren et al., 1999; Tan et al., 1994). A high resolution structure of the RAP74/RAP30 dimer has been solved but a structure of TFIIF bound to RNAP II is yet to be solved (Gaiser et al., 2000). During initiation, TFIIF assists TFIIB in recruiting RNAP II and promotes first phosphodiester bond synthesis as well as helping with promoter escape (Gaiser et al., 2000; Tan et al., 1995). TFIIF may also help untwist the double stranded DNA (Ren et al., 1999). After promotor escape, TFIIF assists in enhancing elongation by suppressing pausing and increasing the rate of elongation (Elmendorf et al., 2001; Funk et al., 2002; Lei et al., 1999; Lei et al., 1998; Ren et al., 1999; Tan et al., 1994; Tan et al., 1995). The exact mechanism of how TFIIF enhances elongation rates and suppresses pausing is not determined. The possibility of TFIIF suppressing pausing by preventing nascent RNA from being displaced out of the active site has been considered (Elmendorf et al., 2001). Preventing RNA slippage out of the active site results in a TFIIF supported active elongation complex with decreased sensitivity to TFIIS-mediated cleavage (Elmendorf et al., 2001; Lei et al., 1999; Renner et al., 2001; Tan et al., 1995). In addition to suppressing pausing, TFIIF

has been observed to increase the rate of pyrophosphorolysis, a reverse reaction of RNA synthesis. The ability of TFIIF to increase the rate of elongation is thought to be the reason for the increase in pyrophosphorolysis (Wang and Hawley, 1993).

Eukaryotic elongation factor TFIIS

Transcription factor IIS, an analogue of bacterial Gre factors, is a general elongation factor for eukaryotic RNAP II, and is known as a transcription factor that can cleave paused or stalled elongation complexes (Fish and Kane, 2002; Gu and Reines, 1995; Rudd et al., 1994). Dinucleotide cleavage is common in paused or stalled complexes. Larger endonucleolytic cleavage products are released when TFIIS acts on arrested complexes (Gu and Reines, 1995; Rudd et al., 1994). Structures of TFIIS bound to yeast RNAP II have been solved by the Cramer lab (Kettenberger et al., 2003, 2004). Domain II and III of TFIIS are required to bind to RNAP and domain III is required for TFIIS-mediated cleavage activities. While domain II of TFIIS binds to the Jaw domain of polymerase II, near the Rpb9 subunit, domain III inserts into and makes contact with residues within the secondary pore of the enzyme (Figure 1.2). Because TFIIS partially blocks the secondary pore, based on general knowledge of NTP substrates entering the enzyme through the secondary pore into the active site, hindered substrate loading is expected (Figure 1.2B) (Cramer et al., 2001; Westover et al., 2004a).

Figure 1.2 **Binding of TFIIS to RNA polymerase II.** Electrostatic picture is shown for yeast RNA polymerase II with red representing negatively charged and blue representing positively charged surfaces. A) RNA polymerase II looking into the active site through the secondary pore. Cyan color ball represents Mg-A in the active site. B) RNA polymerase II with TFIIS (green) bound. Yeast RNA polymerase II structure 1Y1V was downloaded from www.pdb.org. Images were taken after electrostatic calculation by utilizing the PyMol molecular graphics system.

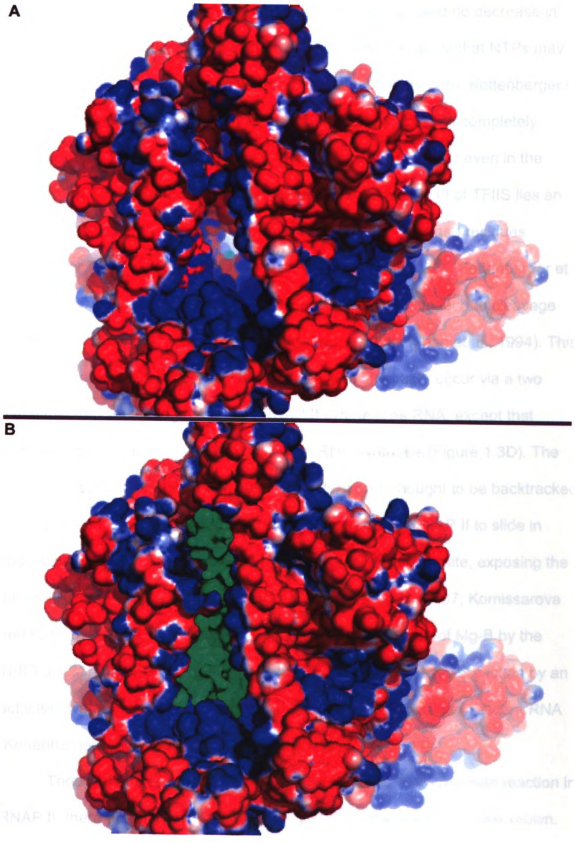

Figure 1.2

However, unpublished kinetic data from the Burton lab showed no decrease in the rate of NTP loading in the presence of TFIIS, which suggest that NTPs may enter the RNAP II through a route other than the secondary pore. Kettenberger et al states that though TFIIS limits the secondary pore, it does not completely occlude it and there is enough room for a substrate NTP to enter even in the presence of TFIIS (Kettenberger et al., 2003). Within domain III of TFIIS lies an acidic hairpin loop which contains invariant D261-E262 (in yeast) residues required for TFIIS-mediated cleavage activity (Jeon et al., 1994; Kettenberger et al., 2003). Even very conservative D261E or E262D mutation lead to cleavage inactivity, which show the importance of the two residues (Jeon et al., 1994). This TFIIS-mediated endonucleolytic cleavage reaction is thought occur via a two metal mechanism analogous to how RNAP II synthesizes RNA, except that endonucleolytic cleavage results rather than RNA synthesis (Figure 1.3D). The majority of paused or stalled elongation complexes are thought to be backtracked (Galburt et al., 2007; Kireeva et al., 2005), which requires RNAP II to slide in such way that the 3'-end of the RNA protrudes from the active site, exposing the internal RNA sequence within the active site (Galburt et al., 2007; Komissarova and Kashlev, 1997a, b). Figure 1.3D shows how coordination of Mg-B by the TFIIS acidic hairpin loop in the active site can lead to an S_N2 type reaction by an activated water molecule on the internal phosphate residue of the nascent RNA (Kettenberger et al., 2003; Sosunov et al., 2003).

Though TFIIS is well known to catalyze a dinucleotide cleavage reaction in RNAP II, there are other important aspects of TFIIS that are not as well known.

Figure 1.3 **Proposed active site mechanisms.** A) Mechanism of phosphodiester bond synthesis. B) Mechanism of pyrophosphorolysis. C) Mechanism of pyrophosphate-mediated endonucleolytic cleavage. D) Mechanism of TFIIS-mediated endonucleolytic cleavage. B = any A, G, C, U nitrogenous base, N = any nucleotide, Mg = magnesium ion, P = phosphate molecule, Glu and Asp = amino acids glutamate and aspartate respectively.

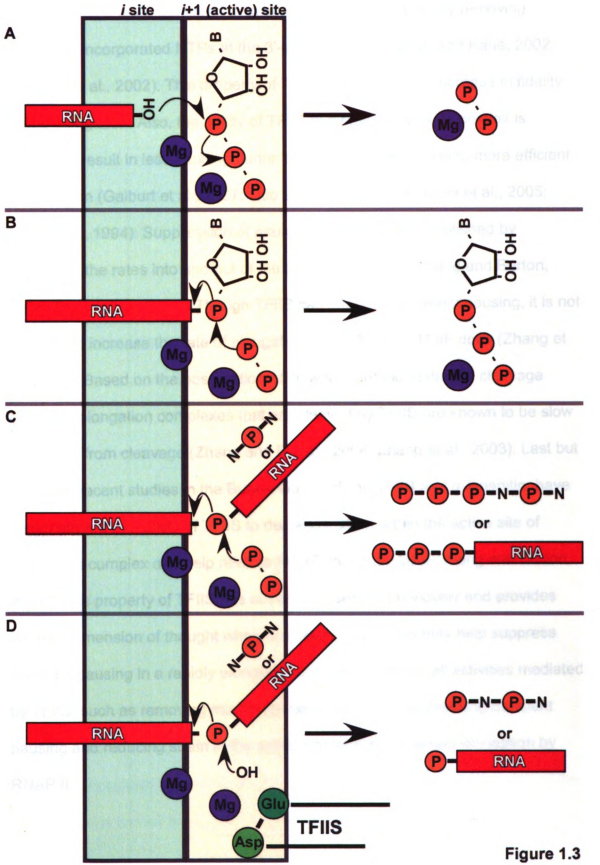

Figure 1.3

First, TFIIS has been observed to suppress misincorporation by removing incorrectly incorporated NTPs at the 3'-end of the RNA (Fish and Kane, 2002; Sijbrandi et al., 2002). This property of TFIIS may lead to an increase in fidelity during elongation. Also, the ability of TFIIS to cleave a paused complex is thought to result in less pausing during elongation, which leads to more efficient transcription (Galburt et al., 2007; Guo and Price, 1993; Kireeva et al., 2005; Rudd et al., 1994). Suppression of pausing by TFIIS is accomplished by enhancing the rates into and out of the pausing pathway (Zhang and Burton, 2004; Zhang et al., 2003). Though TFIIS can suppress transient pausing, it is not believed to increase the rate of elongation by RNAP II as TFIIF does (Zhang et al., 2003). Based on the observation of slow forward elongation of cleavage products, elongation complexes that are cleaved by TFIIS are known to be slow to recover from cleavage (Zhang and Burton, 2004; Zhang et al., 2003). Last but not least, recent studies in the Burton lab, involving TFIIS and α-amanitin, have demonstrated the ability of TFIIS to decrease strain within the active site of elongation complex and help release PPi (Gong et al., 2005; Xiong and Burton, 2007). This property of TFIIS has not been observed previously and provides another dimension of thought when describing how TFIIS may help suppress transient pausing in a rapidly elongating complex. Perhaps all activities mediated by TFIIS, such as removing misincorporated products, suppressing transient pausing and reducing strain in the active site lead to enhanced elongation by RNAP II.

Pyrophosphate and the mechanism of multi-subunit RNA polymerase

Pyrophosphate, also known as diphosphate or inorganic pyrophosphate is the product released following phosphodiester bond synthesis and in higher concentrations, can mediate a reverse polymerization reaction known as pyrophosphorolysis (Bengal et al., 1991; Chafin et al., 1995; Rozovskaya et al., 1984; Rudd et al., 1994; Sosunov et al., 2003). PPi can penetrate the active site of multi-subunit RNAP and bind to the pre-translocated elongation complex, in which the enzyme has completed the phosphodiester bond synthesis but has not translocated forward to vacate the active site for another substrate NTP to enter (Kashkina et al., 2006; Svetlov et al., 2007). Because of the ability of PPi to bind pre-translocated elongation complex (while NTPs bind to the post-translocated elongation complex), PPi can be utilized as a dynamic probe to study the core mechanism of multi-subunit RNAP. Once bound to the pre-translocated elongation complex, PPi can do one of two things. First, it can drive the reverse RNA synthesis reaction, leading to release in nucleoside triphosphates (or oligo nucleotides after endonucleolytic cleavage). Second, as we describe in the second chapter, it may bind and hold the polymerase in a product complex, helping the elongation complex to remain on the active synthesis pathway. In order to drive the reverse reaction, a high concentration of PPi (mM concentrations) is required (Rudd et al., 1994). A possible mechanism of pyrophosphorolysis has been characterized in detail in the past. Pyrophosphorolysis relies on a two Mg^{2+} mechanism within the active site of the RNAP. This is similar but not equal to hydrolysis or TFIIS-mediated cleavage. As

shown in Figure 1.3B, PPi bound to pre-translocated elongation complex in the active site can coordinate Mg-B in a similar manner to that in which the triphosphate tail of an NTP can coordinate Mg-B during synthesis. Coordination of two Mg^{2+}, PPi and the phosphorus atom of RNA increases the electrophilicity of the RNA phosphorus atom while increasing the nucleophilicity of the attacking PPi. This leads to pyrophosphorolysis and release of NTP (Chafin et al., 1995; Rozovskaya et al., 1984; Rudd et al., 1994; Sosunov et al., 2003). The release of nucleotides with triphosphate is different from water-mediated hydrolysis, which releases NMPs (Sosunov et al., 2003).

Not only is PPi involved in a reverse RNA synthesis reaction, it is also involved in other aspects of transcription (or replication) such as oligonucleotide cleavage reactions and fidelity. As mentioned earlier, TFIIS catalyzes endonucleolytic cleavage reactions, either in dinucleotide or oligonucleotide increments in paused and arrested elongation complexes respectively (Gu and Reines, 1995; Rudd et al., 1994). Similar to TFIIS, PPi cleaves arrested complexes in oligonucleotide increments. The mechanism is similar to pyrophosphorolysis except a backtracked RNA exposes an internal RNA sequence in the active site, which results in release of larger RNA fragments after cleavage. Figure 1.3C show details of PPi-mediated cleavage on backtracked RNA and the release of oligonucleotides (Rudd et al., 1994; Sosunov et al., 2003). Although endonucleolytic reactions can appear similar between PPi and TFIIS, resulting cleavage products are slightly different (compare Figure 1.3C and D). PPi-mediated cleavage releases an

oligonucleotide with an intact triphosphate tail while TFIIS-mediated cleavage products have a monophosphate tail (Rudd et al., 1994; Sosunov et al., 2003).

Yet another possible PPi involvement in polymerase mechanism is fidelity. Though it has not been observed in eukaryotic RNAP II, PPi has been shown to decrease incorporation and extension of incorrect NTPs (or dNTPs) in simple, generally single subunit DNA polymerases and bacterial RNAPs, resulting in increased enzyme fidelity (Kahn and Hearst, 1989; Lecomte et al., 1986; Vaisman et al., 2005). An exact mechanism of how PPi inhibits misincorporation is not known. However, it is thought that PPi may inhibit misincorporation through pyrophosphorolysis (Kahn and Hearst, 1989; Lecomte et al., 1986; Vaisman et al., 2005). Although it has not been described, another possibility is that PPi may inhibit misincorporation by inhibiting RNA synthesis in the first place, either by competing with NTP entry by holding the elongation complex in the product complex (occupying the active site) or by inhibiting the movement of NTPs from a pre-insertion site to an insertion (catalytic) site.

The elongation mechanism in multi-subunit RNA polymerases

NTP-driven translocation and main enzyme channel loading

The core mechanism of multi-subunit RNAPs has long been debated and we are yet to converge upon a unified mechanism for transcription elongation. The first mechanism that will be discussed will be NTP-driven translocation (Burton et al., 2005; Gong et al., 2004; Gong et al., 2005; Langelier et al., 2005; Nedialkov et al., 2003; Xiong and Burton, 2007; Zhang and Burton, 2004; Zhang

et al., 2003; Zhang et al., 2005). This mechanism was proposed in 2003 because of apparent inconsistencies in the then dominant secondary pore NTP loading/ thermal ratchet translocation mechanism. In the NTP-driven translocation model, the translocation state of the elongation complex need not matter for NTP loading because NTPs can load to either the pre- or post-translocated states. This is important because kinetic data from Burton lab appeared most consistent with RNAP being able to utilize both pre- and post-translocated states for loading NTPs (Gong et al., 2004; Nedialkov et al., 2003). As discussed below, based on the thermal ratchet mechanism, a pre-translocated elongation complex, in which the 3'-end of the RNA occupies the active site, cannot successfully load substrate NTPs until translocation occurs (Kashkina et al., 2006). Because NTPs cannot load to the pre-translocated elongation complex according to a thermal ratchet mechanism, the NTP-driven translocation mechanism seems more likely if NTPs bind both elongation states.

According to the NTP-driven translocation model, NTPs load through the main enzyme channel (Figure 1.4). In this manner, NTPs can load to the pre-translocated elongation complex. Such a mechanism also might enhance the enzyme's fidelity through the pre-screening of NTPs (Gong et al., 2005; Xiong and Burton, 2007). Utilizing α-amanitin, a potent translocation inhibitor, the Burton lab demonstrated the presence and effects of templated downstream NTPs.

Figure 1.4 **Two NTP loading mechanisms.** Arrows indicate main enzyme channel (upper) and secondary pore (lower) loading hypotheses. Red colored NTP shows relative location of the active site. This figure was created by utilizing the PyMol molecular graphics system. Crystal structure 1R9S was downloaded from www.pdb.org.

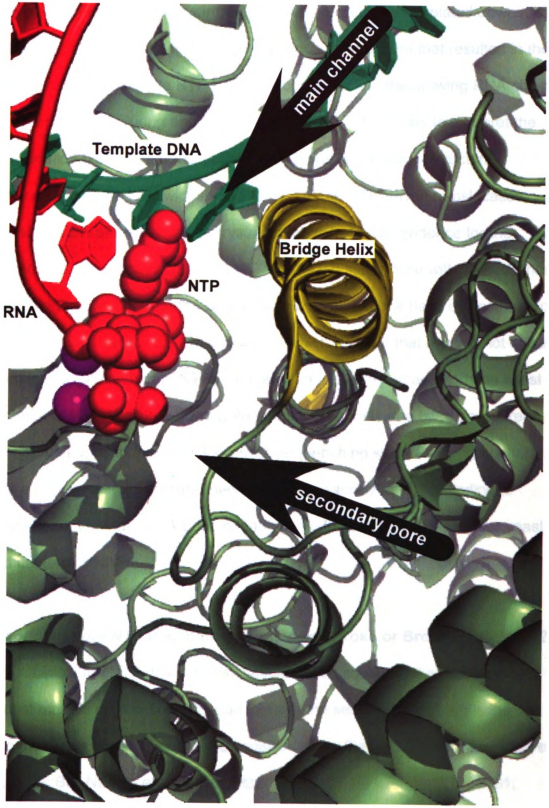
main channel
Template DNA
Bridge Helix
NTP
RNA
secondary pore

Figure 1.4

With α-amanitin blocking forward translocation, accurately templated downstream NTPs were shown to provide forward translocation pressure that resulted in the expulsion of an active site NTP fated to incorporate into the growing RNA chain (Gong et al., 2005; Xiong and Burton, 2007). RNAP II appears to interpret the translocation block as a transcription error. However, a lack of structural evidence has limited the widespread appeal of the NTP-driven translocation model as none of the published crystal structures provide evidence for the presence of downstream templated NTPs. Also, a study done with fluorescence quenching has shown that the DNA template is melted one base downstream of the active site at a time for yeast RNAP II, which suggest that there is not enough room to pre-load substrate NTPs (Kashkina et al., 2007). In addition, the latest bacterial RNAP structure shows DNA separation of only one base downstream of the active site, confirming the fluorescence quenching study (Vassylyev et al., 2007a). These results together decrease the possibility of NTPs binding to downstream template DNA prior to loading into the active site at least for yeast and bacterial RNAPs.

Secondary pore NTP loading models: Power-stroke or Brownian Ratchet?

Unlike the NTP driven translocation model, power-stroke and thermal ratchet models require NTPs to load through the secondary pore while the enzyme is in a post-translocated elongation state (Figure 1.4) (Abbondanzieri et al., 2005; Bar-Nahum et al., 2005; Batada et al., 2004; Cramer et al., 2001; Kashkina et al., 2007; Kashkina et al., 2006; Landick, 2005; Westover et al.,

2004a; Yin and Steitz, 2004). In the power-stroke mechanism, energy and needed conformational changes for translocation and DNA strand separation are derived from phosphodiester bond synthesis and PPi release. A power-stroke mechanism requires tight coupling of energy generation from NTP hydrolysis and translocation of the enzyme (Wang and Oster, 2002; Yin and Steitz, 2004). The power-stroke has been discussed in single subunit RNAPs while it has not been mentioned for multi-subunit RNAPs. Further studies from different laboratories revealed more evidence in support of a thermal ratchet mechanism for both single and multi-subunit RNAPs as pre- and post-translocated elongation complexes appeared to interconvert prior to binding a substrate (Bar-Nahum et al., 2005; Guo and Sousa, 2006; Kashkina et al., 2006).

Brownian ratchet, also known as the thermal ratchet mechanism is a more widely accepted mechanism that involves loading of NTPs through the secondary pore. It differs from the power-stroke in the sense that NTP hydrolysis is not required for the elongation complex to translocate forward. In fact, this mechanism proposes that multiple translocation states co-exist at the same time as pre- and post-translocated elongation complexes in equilibrium (Bar-Nahum et al., 2005; Guo and Sousa, 2006; Kashkina et al., 2006). Knowing that only pre-translocated elongation complex is sensitive to PPi, Kashkina et al. demonstrated the significance of PPi in determining the translocation mechanism by showing that only some elongation complexes are sensitive to pyrophosphorolysis and the sensitivity changed based on the length of the DNA/RNA hybrid. This is consistent with the idea that both pre- and post-translocated elongation states

are in equilibrium, and the equilibrium can shift based on the length of the DNA/RNA hybrid or binding of NTP or PPi (Kashkina et al., 2006). Others have argued for the thermal ratchet mechanism based on pre-steady state kinetic studies (Anand and Patel, 2006; Arnold and Cameron, 2004; Arnold et al., 2004; Bar-Nahum et al., 2005). Even with overwhelming support, there are potential weaknesses in this model that must be addressed. The secondary pore of multi-subunit RNAP is a very narrow, negatively charged channel that should inhibit the entrance of highly negatively charged NTPs (Batada et al., 2004). It seems unlikely that the secondary pore can allow NTP entry, TFIIS entry, PPi release as well as dynamic trigger loop motions simultaneously. Also, α-amanitin is thought to block the secondary pore when bound to RNAP II. This however, does not influence the synthesis of the first phosphodiester bond synthesis when α - amanitin and NTPs are added together (Chafin et al., 1995; Gong et al., 2004). These are some of the questions that must be addressed to strengthen the thermal ratchet mechanism.

The trigger loop closing theory, which coincides with the thermal ratchet model, is the newest addition to the secondary pore loading mechanism. As shown in Figure 1.5, recently solved high resolution crystal structures published by Kornberg (for eukaryotic) and Vassylyev (for prokaryotic) laboratories have shown the possibility of the trigger loop playing an important role in isomerization and phosphodiester bond synthesis (Vassylyev et al., 2007b; Wang et al., 2006). With correctly templated NTP in the A (addition) site, the trigger loop is able to close the active site and stabilize the NTP for phosphodiester bond synthesis.

Figure 1.5 **RNA polymerase active site dynamics.** Closed trigger loop structure, which is displayed with important residues listed. A) *Thermus thermophilus* active site (PDB code: 2O5J) B) *Saccharomyces cerevisiae* active site (PDB code: 2E2H). Structures were viewed and images were created by utilizing the PyMol molecular graphics system.

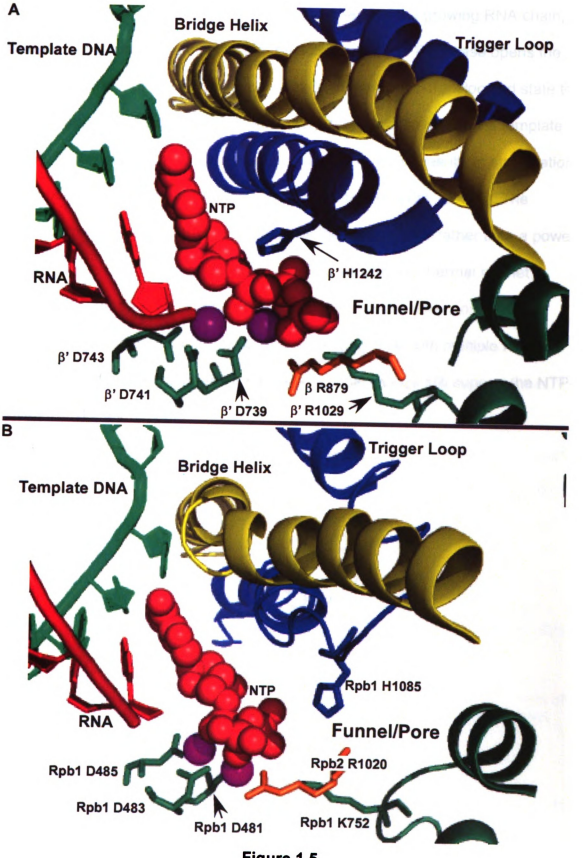
A
Template DNA
Bridge Helix
Trigger Loop
NTP
RNA
β' H1242
Funnel/Pore
β' D743
β' D741
β' D739
β R879
β' R1029
B
Template DNA
Bridge Helix
Trigger Loop
NTP
RNA
Rpb1 H1085
Funnel/Pore
Rpb1 D485
Rpb2 R1020
Rpb1 D483
Rpb1 D481
Rpb1 K752

Figure 1.5

Once an NMP has been incorporated into the 3'-end of the growing RNA chain, disruption of the contact points within the active site and PPi release opens the trigger loop and moves elongation complex from closed/pre-translocated state to an open/post-translocated state. Presumably, translocation occurs via template sliding. RNAP can then bind another substrate NTP, which results in stabilization of the post-translocated elongation complex (Vassylyev et al., 2007b). The proposed mechanism for translocation is via thermal motions rather than a power stroke. Though current crystallographic studies support the thermal ratchet mechanism and one NTP loading per translocation cycle, other possible mechanisms such as the NTP-driven translocation model with multiple NTP loading should not be dismissed because functional assays still support the NTP-driven translocation model.

REFERENCES

Abbondanzieri, E.A., Greenleaf, W.J., Shaevitz, J.W., Landick, R., and Block, S.M. (2005). Direct observation of base-pair stepping by RNA polymerase. Nature *438*, 460-465.

Anand, V.S., and Patel, S.S. (2006). Transient state kinetics of transcription elongation by T7 RNA polymerase. J Biol Chem *281*, 35677-35685.

Arnold, J.J., and Cameron, C.E. (2004). Poliovirus RNA-dependent RNA polymerase (3Dpol): pre-steady-state kinetic analysis of ribonucleotide incorporation in the presence of Mg2+. Biochemistry *43*, 5126-5137.

Arnold, J.J., Gohara, D.W., and Cameron, C.E. (2004). Poliovirus RNA-dependent RNA polymerase (3Dpol): pre-steady-state kinetic analysis of ribonucleotide incorporation in the presence of Mn2+. Biochemistry *43*, 5138-5148.

Artsimovitch, I., and Vassylyev, D.G. (2006). Is it easy to stop RNA polymerase? Cell Cycle *5*, 399-404.

Bar-Nahum, G., Epshtein, V., Ruckenstein, A.E., Rafikov, R., Mustaev, A., and Nudler, E. (2005). A ratchet mechanism of transcription elongation and its control. Cell *120*, 183-193.

Batada, N.N., Westover, K.D., Bushnell, D.A., Levitt, M., and Kornberg, R.D. (2004). Diffusion of nucleoside triphosphates and role of the entry site to the RNA polymerase II active center. Proc Natl Acad Sci USA *101*, 17361-17364.

Bengal, E., Flores, O., Krauskopf, A., Reinberg, D., and Aloni, Y. (1991). Role of the mammalian transcription factors IIF, IIS, and IIX during elongation by RNA polymerase II. Mol Cell Biol *11*, 1195-1206.

Burton, Z.F., Feig, M., Gong, X.Q., Zhang, C., Nedialkov, Y.A., and Xiong, Y. (2005). NTP-driven translocation and regulation of downstream template opening by multi-subunit RNA polymerases. Biochem Cell Biol *83*, 486-496.

Bushnell, D.A., Cramer, P., and Kornberg, R.D. (2002). Structural basis of transcription: alpha-amanitin-RNA polymerase II cocrystal at 2.8 A resolution. Proc Natl Acad Sci USA *99*, 1218-1222.

Chafin, D.R., Guo, H., and Price, D.H. (1995). Action of alpha-amanitin during pyrophosphorolysis and elongation by RNA polymerase II. J Biol Chem *270*, 19114-19119.

Choder, M. (2004). Rpb4 and Rpb7: subunits of RNA polymerase II and beyond. Trends Biochem Sci *29*, 674-681.

Conaway, J.W., and Conaway, R.C. (1999). Transcription elongation and human disease. Annu Rev Biochem *68*, 301-319.

Coulombe, B., and Burton, Z.F. (1999). DNA bending and wrapping around RNA polymerase: a "revolutionary" model describing transcriptional mechanisms. Microbiol Mol Biol Rev *63*, 457-478.

Cramer, P. (2004). RNA polymerase II structure: from core to functional complexes. Curr Opin Genet Dev *14*, 218-226.

Cramer, P., Bushnell, D.A., and Kornberg, R.D. (2001). Structural basis of transcription: RNA polymerase II at 2.8 angstrom resolution. Science *292*, 1863-1876.

Ebright, R.H. (2000). RNA polymerase: structural similarities between bacterial RNA polymerase and eukaryotic RNA polymerase II. J Mol Biol *304*, 687-698.

Edwards, A.M., Kane, C.M., Young, R.A., and Kornberg, R.D. (1991). Two dissociable subunits of yeast RNA polymerase II stimulate the initiation of transcription at a promoter in vitro. J Biol Chem *266*, 71-75.

Elmendorf, B.J., Shilatifard, A., Yan, Q., Conaway, J.W., and Conaway, R.C. (2001). Transcription factors TFIIF, ELL, and Elongin negatively regulate SII-induced nascent transcript cleavage by non-arrested RNA polymerase II elongation intermediates. J Biol Chem *276*, 23109-23114.

Fish, R.N., and Kane, C.M. (2002). Promoting elongation with transcript cleavage stimulatory factors. Biochim Bophys Acta *1577*, 287-307.

Funk, J.D., Nedialkov, Y.A., Xu, D., and Burton, Z.F. (2002). A key role for the alpha 1 helix of human RAP74 in the initiation and elongation of RNA chains. J Biol Chem *277*, 46998-47003.

Gaiser, F., Tan, S., and Richmond, T.J. (2000). Novel dimerization fold of RAP30/RAP74 in human TFIIF at 1.7 A resolution. J Mol Biol *302*, 1119-1127.

Galburt, E.A., Grill, S.W., Wiedmann, A., Lubkowska, L., Choy, J., Nogales, E., Kashlev, M., and Bustamante, C. (2007). Backtracking determines the force sensitivity of RNAP II in a factor-dependent manner. Nature *446*, 820-823.

Gnatt, A.L., Cramer, P., Fu, J., Bushnell, D.A., and Kornberg, R.D. (2001). Structural basis of transcription: an RNA polymerase II elongation complex at 3.3 A resolution. Science *292*, 1876-1882.

Gong, X.Q., Nedialkov, Y.A., and Burton, Z.F. (2004). Alpha-amanitin blocks translocation by human RNA polymerase II. J Biol Chem *279*, 27422-27427.

Gong, X.Q., Zhang, C., Feig, M., and Burton, Z.F. (2005). Dynamic error correction and regulation of downstream bubble opening by human RNA polymerase II. Mol Cell *18*, 461-470.

Gu, W., and Reines, D. (1995). Variation in the size of nascent RNA cleavage products as a function of transcript length and elongation competence. J Biol Chem *270*, 30441-30447.

Guo, H., and Price, D.H. (1993). Mechanism of DmS-II-mediated pause suppression by Drosophila RNA polymerase II. J Biol Chem *268*, 18762-18770.

Guo, Q., and Sousa, R. (2006). Translocation by T7 RNA polymerase: a sensitively poised Brownian ratchet. J Mol Biol *358*, 241-254.

Jeon, C., Yoon, H., and Agarwal, K. (1994). The transcription factor TFIIS zinc ribbon dipeptide Asp-Glu is critical for stimulation of elongation and RNA cleavage by RNA polymerase II. Proc Natl Acad Sci USA *91*, 9106-9110.

Kahn, J.D., and Hearst, J.E. (1989). Reversibility of nucleotide incorporation by Escherichia coli RNA polymerase, and its effect on fidelity. J Mol Biol *205*, 291-314.

Kashkina, E., Anikin, M., Brueckner, F., Lehmann, E., Kochetkov, S.N., McAllister, W.T., Cramer, P., and Temiakov, D. (2007). Multisubunit RNA polymerases melt only a single DNA base pair downstream of the active site. J Biol Chem *282*, 21578-21582.

Kashkina, E., Anikin, M., Tahirov, T.H., Kochetkov, S.N., Vassylyev, D.G., and Temiakov, D. (2006). Elongation complexes of Thermus thermophilus RNA polymerase that possess distinct translocation conformations. Nucleic Acids Res *34*, 4036-4045.

Kettenberger, H., Armache, K.J., and Cramer, P. (2003). Architecture of the RNA polymerase II-TFIIS complex and implications for mRNA cleavage. Cell *114*, 347-357.

Kettenberger, H., Armache, K.J., and Cramer, P. (2004). Complete RNA polymerase II elongation complex structure and its interactions with NTP and TFIIS. Mol Cell *16*, 955-965.

Kireeva, M.L., Hancock, B., Cremona, G.H., Walter, W., Studitsky, V.M., and Kashlev, M. (2005). Nature of the nucleosomal barrier to RNA polymerase II. Mol Cell *18*, 97-108.

Komissarova, N., and Kashlev, M. (1997a). RNA polymerase switches between inactivated and activated states By translocating back and forth along the DNA and the RNA. J Biol Chem *272*, 15329-15338.

Komissarova, N., and Kashlev, M. (1997b). Transcriptional arrest: Escherichia coli RNA polymerase translocates backward, leaving the 3' end of the RNA intact and extruded. Proc Natl Acad Sci USA *94*, 1755-1760.

Landick, R. (2001). RNA polymerase clamps down. Cell *105*, 567-570.

Landick, R. (2004). Active-site dynamics in RNA polymerases. Cell *116*, 351-353.

Landick, R. (2005). NTP-entry routes in multi-subunit RNA polymerases. Trends Biochem Sci *30*, 651-654.

Langelier, M.F., Baali, D., Trinh, V., Greenblatt, J., Archambault, J., and Coulombe, B. (2005). The highly conserved glutamic acid 791 of Rpb2 is

involved in the binding of NTP and Mg(B) in the active center of human RNA polymerase II. Nucleic Acids Res *33*, 2629-2639.

Lecomte, P., Doubleday, O.P., and Radman, M. (1986). Evidence for an intermediate in DNA synthesis involving pyrophosphate exchange. A possible role in fidelity. J Mol Biol *189*, 643-652.

Lei, L., Ren, D., and Burton, Z.F. (1999). The RAP74 subunit of human transcription factor IIF has similar roles in initiation and elongation. Mol Cell Biol *19*, 8372-8382.

Lei, L., Ren, D., Finkelstein, A., and Burton, Z.F. (1998). Functions of the N- and C-terminal domains of human RAP74 in transcriptional initiation, elongation, and recycling of RNA polymerase II. Mol Cell Biol *18*, 2130-2142.

Mooney, R.A., Darst, S.A., and Landick, R. (2005). Sigma and RNA polymerase: an on-again, off-again relationship? Mol Cell *20*, 335-345.

Nedialkov, Y.A., Gong, X.Q., Hovde, S.L., Yamaguchi, Y., Handa, H., Geiger, J.H., Yan, H., and Burton, Z.F. (2003). NTP-driven translocation by human RNA polymerase II. J Biol Chem *278*, 18303-18312.

Nikolov, D.B., and Burley, S.K. (1997). RNA polymerase II transcription initiation: a structural view. Proc Natl Acad Sci USA *94*, 15-22.

Ren, D., Lei, L., and Burton, Z.F. (1999). A region within the RAP74 subunit of human transcription factor IIF is critical for initiation but dispensable for complex assembly. Mol Cell Biol *19*, 7377-7387.

Renner, D.B., Yamaguchi, Y., Wada, T., Handa, H., and Price, D.H. (2001). A highly purified RNA polymerase II elongation control system. J Biol Chem *276*, 42601-42609.

Rozovskaya, T.A., Rechinsky, V.O., Bibilashvili, R.S., Karpeisky, M., Tarusova, N.B., Khomutov, R.M., and Dixon, H.B. (1984). The mechanism of pyrophosphorolysis of RNA by RNA polymerase. Endowment of RNA polymerase with artificial exonuclease activity. Biochem J *224*, 645-650.

Rudd, M.D., Izban, M.G., and Luse, D.S. (1994). The active site of RNA polymerase II participates in transcript cleavage within arrested ternary complexes. Proc Natl Acad Sci USA *91*, 8057-8061.

Shilatifard, A. (1998a). Factors regulating the transcriptional elongation activity of RNA polymerase II. Faseb J *12*, 1437-1446.

Shilatifard, A. (1998b). The RNA polymerase II general elongation complex. Biol Chem *379*, 27-31.

Sijbrandi, R., Fiedler, U., and Timmers, H.T. (2002). RNA polymerase II complexes in the very early phase of transcription are not susceptible to TFIIS-induced exonucleolytic cleavage. Nucleic Acids Res *30*, 2290-2298.

Sosunov, V., Sosunova, E., Mustaev, A., Bass, I., Nikiforov, V., and Goldfarb, A. (2003). Unified two-metal mechanism of RNA synthesis and degradation by RNA polymerase. EMBO J *22*, 2234-2244.

Steitz, T.A. (1998). A mechanism for all polymerases. Nature *391*, 231-232.

Svetlov, V., Belogurov, G.A., Shabrova, E., Vassylyev, D.G., and Artsimovitch, I. (2007). Allosteric control of the RNA polymerase by the elongation factor RfaH. Nucleic Acids Res *35*, 5694-5705.

Sweetser, D., Nonet, M., and Young, R.A. (1987). Prokaryotic and eukaryotic RNA polymerases have homologous core subunits. Proc Natl Acad Sci USA *84*, 1192-1196.

Tan, S., Aso, T., Conaway, R.C., and Conaway, J.W. (1994). Roles for both the RAP30 and RAP74 subunits of transcription factor IIF in transcription initiation and elongation by RNA polymerase II. J Biol Chem *269*, 25684-25691.

Tan, S., Conaway, R.C., and Conaway, J.W. (1995). Dissection of transcription factor TFIIF functional domains required for initiation and elongation. Proc Natl Acad Sci USA *92*, 6042-6046.

Vaisman, A., Ling, H., Woodgate, R., and Yang, W. (2005). Fidelity of Dpo4: effect of metal ions, nucleotide selection and pyrophosphorolysis. EMBO J *24*, 2957-2967.

Van Wynsberghe, A., Li, G., and Cui, Q. (2004). Normal-mode analysis suggests protein flexibility modulation throughout RNA polymerase's functional cycle. Biochemistry *43*, 13083-13096.

Vassylyev, D.G., Sekine, S., Laptenko, O., Lee, J., Vassylyeva, M.N., Borukhov, S., and Yokoyama, S. (2002). Crystal structure of a bacterial RNA polymerase holoenzyme at 2.6 A resolution. Nature *417*, 712-719.

Vassylyev, D.G., Vassylyeva, M.N., Perederina, A., Tahirov, T.H., and Artsimovitch, I. (2007a). Structural basis for transcription elongation by bacterial RNA polymerase. Nature *448*, 157-162.

Vassylyev, D.G., Vassylyeva, M.N., Zhang, J., Palangat, M., Artsimovitch, I., and Landick, R. (2007b). Structural basis for substrate loading in bacterial RNA polymerase. Nature *448*, 163-168.

Villain-Guillot, P., Bastide, L., Gualtieri, M., and Leonetti, J.P. (2007). Progress in targeting bacterial transcription. Drug Discovery Today *12*, 200-208.

von Hippel, P.H. (1998). An integrated model of the transcription complex in elongation, termination, and editing. Science *281*, 660-665.

Wang, D., Bushnell, D.A., Westover, K.D., Kaplan, C.D., and Kornberg, R.D. (2006). Structural basis of transcription: role of the trigger loop in substrate specificity and catalysis. Cell *127*, 941-954.

Wang, D., and Hawley, D.K. (1993). Identification of a 3'-->5' exonuclease activity associated with human RNA polymerase II. Proc Natl Acad Sci USA *90*, 843-847.

Wang, H., and Oster, G. (2002). Ratchets, power strokes, and molecular motors. Applied Physics A *75*, 315-323.

Westover, K.D., Bushnell, D.A., and Kornberg, R.D. (2004a). Structural basis of transcription: nucleotide selection by rotation in the RNA polymerase II active center. Cell *119*, 481-489.

Westover, K.D., Bushnell, D.A., and Kornberg, R.D. (2004b). Structural basis of transcription: separation of RNA from DNA by RNA polymerase II. Science *303*, 1014-1016.

Xiong, Y., and Burton, Z.F. (2007). A Tunable Ratchet Driving Human RNA Polymerase II Translocation Adjusted by Accurately Templated Nucleoside Triphosphates Loaded at Downstream Sites and by Elongation Factors. J Biol Chem *282*, 36582-36592.

Yin, Y.W., and Steitz, T.A. (2004). The structural mechanism of translocation and helicase activity in T7 RNA polymerase. Cell *116*, 393-404.

Zhang, C., and Burton, Z.F. (2004). Transcription factors IIF and IIS and nucleoside triphosphate substrates as dynamic probes of the human RNA polymerase II mechanism. J Mol Biol *342*, 1085-1099.

Zhang, C., Yan, H., and Burton, Z.F. (2003). Combinatorial control of human RNA polymerase II (RNAP II) pausing and transcript cleavage by transcription factor IIF, hepatitis delta antigen, and stimulatory factor II. J Biol Chem *278*, 50101-50111.

Zhang, C., Zobeck, K.L., and Burton, Z.F. (2005). Human RNA polymerase II elongation in slow motion: role of the TFIIF RAP74 alpha1 helix in nucleoside triphosphate-driven translocation. Mol Cell Biol *25*, 3583-3595.

Zhang, G., Campbell, E.A., Minakhin, L., Richter, C., Severinov, K., and Darst, S.A. (1999). Crystal structure of Thermus aquaticus core RNA polymerase at 3.3 A resolution. Cell *98*, 811-824.

Chapter 2

Pyrophosphate as a dynamic probe of the human RNA polymerase II mechanism

Summary

Pyrophosphorolysis is the reverse of the RNA synthesis reaction, in which pyrophosphate (PPi) interacts with the pre-translocated elongation complex to remove the 3'-NMP (nucleoside monophosphate) from a nascent RNA chain to release NTP (nucleoside triphosphate). PPi can also induce apparent cleavage of a dinucleotide, in a reaction that mimics dinucleotide cleavage stimulated by Transcription Factor IIS (TFIIS). PPi suppresses transcriptional pausing, presumably by retaining the elongation complex on the active synthesis pathway. PPi does not inhibit the chemical step of TFIIS-mediated dinucleotide cleavage, but PPi blocks formation of off-pathway complexes that are sensitive to TFIIS. When added together with NTP substrates, PPi inhibits elongation, particularly at low NTP concentrations. Approaching a stall position, conditions can be obtained in which the reverse reaction through pyrophosphorolysis balances forward synthesis. Addition of the next templated substrate NTP results in generation of longer products, showing that delayed complexes are not arrested but, rather, remain elongation competent. Because pre- and post-translocation states exist in dynamic equilibrium at a stall, translocation progresses via a sliding thermal ratchet and/or a pre-selection intermediate, to which both NTP substrates and PPi can bind.

Introduction

X-ray crystal structures of yeast (Sc) RNA polymerase (RNAP) II and bacterial Thermus thermophilus (Tt) RNAP engaged in elongation clarify ideas about NTP loading, translocation, and conformational coupling during each phosphodiester bond addition (Vassylyev et al., 2007; Wang et al., 2006). NTPs are thought to load through the secondary pore to the deeply buried active site (Batada et al., 2004; Cramer et al., 2001; Vassylyev et al., 2007; Westover et al., 2004). From Sc RNAP II structures, NTPs may first interact in the pore with an "entry" site, in which the NTP is associated with active site Mg^{2+} but not yet paired to the DNA template (Sosunov et al., 2003; Wang et al., 2006; Westover et al., 2004). From Tt RNAP structures, NTPs then may move to a pre-insertion or pre-selection position, which is paired to template but not accurately positioned for incorporation. A structural change close to the active site is then believed to occur in which the "trigger loop-trigger helices" assembly tightens on the substrate NTP to form the insertion site structure, which is capable of bond addition (Vassylyev et al., 2007; Wang et al., 2006). Closing of the trigger helices over the active site appears to form specific amino acid contacts with the substrate NTP. After chemistry, it is expected that the trigger helices disorder to form a relaxed trigger loop structure. Relaxation of the trigger loop helps to open the secondary pore, which would be expected to facilitate PPi release and NTP loading. Relaxation of the trigger loop-trigger helices assembly may free the RNA-DNA hybrid and DNA duplex to translocate to the next base position (Vassylyev et al., 2007). It has also been suggested that binding of NTP

substrates to downstream template sites may stimulate translocation (Gong et al., 2004; Gong et al., 2005; Langelier et al., 2005; Nedialkov et al., 2003a; Xiong and Burton, 2007). Because NTPs are thought to bind primarily to the post-translocated elongation complex, however, NTPs can be considered to be a probe of the post-translocated elongation complex (Bar-Nahum et al., 2005; Kashkina et al., 2006; Svetlov et al., 2007; Vassylyev et al., 2007; Wang et al., 2006; Westover et al., 2004).

Human (Hs) RNAP II binds to TFIIF, which strongly stimulates the elongation rate (Funk et al., 2002; Lei et al., 1999; Lei et al., 1998; Ren et al., 1999; Tan et al., 1994; Tan et al., 1995). For the homologous Sc RNAP I, the A49/A34.5 subunit subcomplex, which appears structurally similar to TFIIF, is located close to the "funnel" and Rpb8 subunit, a shared subunit among RNAPs I and II (Kuhn et al., 2007). TFIIF, therefore, may occupy a similar position on RNAP II to A49/A34.5 on RNAP I. The funnel leads to the secondary pore, which is the presumed route for NTP entry (Batada et al., 2004; Cramer et al., 2001; Vassylyev et al., 2007; Westover et al., 2004). Because TFIIF and A49/A34.5 appear to bind to the outside of their respective RNAPs to stimulate elongation within a buried active site (Kuhn et al., 2007), TFIIF and related factors appear to act as allosteric effectors of the catalytic mechanism, altering the RNAP conformation to support catalytic function. In addition to accelerating elongation, TFIIF has been shown to stimulate pyrophosphorolysis by Hs RNAP II (Wang and Hawley, 1993).

Domain III of TFIIS, a Zn^{2+} ribbon, penetrates the secondary pore of RNAP II and projects a conserved Asp-Glu motif toward the active site (Kettenberger et al., 2003, 2004). The Asp-Glu motif is thought to hold a second Mg^{2+} close to the active site Mg^{2+}-A, which is held by a conserved sequence of Asn-Ala-Asp-Phe-Asp-Gly-Asp in Rpb1 (Kettenberger et al., 2003, 2004). TFIIS stimulates dinucleotide cleavage of the nascent RNA within paused complexes, and TFIIS can cleave longer nucleotide fragments from further backtracked and arrested elongation complexes (Fish and Kane, 2002; Galburt et al., 2007; Gu and Reines, 1995; Guo and Price, 1993; Kireeva et al., 2005; Langelier et al., 2005; Rudd et al., 1994; Wang and Hawley, 1993). Because TFIIS cleaves dinucleotides from paused elongation complexes but does not have a large effect on elongation rate (Zhang et al., 2003), TFIIS can be used as a probe for transcriptional pausing. Entry onto the pausing pathway sensitizes the nascent RNA to TFIIS-mediated cleavage (Galburt et al., 2007; Zhang and Burton, 2004; Zhang et al., 2003).

PPi is a by-product of transcription elongation. Acting as a substrate, it can mediate a reverse phosphodiester bond synthesis reaction known as pyrophosphorolysis. Pyrophosphorolysis reactions have been well documented for both RNAPs and DNA polymerases (DNAPs) (Chafin et al., 1995; Rozovskaya et al., 1984; Rudd et al., 1994; Sosunov et al., 2003; Vaisman et al., 2005). Generally, these reactions require high concentrations of exogenous PPi to drive the thermodynamically unfavorable reverse reaction (Rudd et al., 1994). For RNAPs, each pyrophosphorolysis reaction releases a single NTP from the 3'-

end of the nascent RNA chain (Chafin et al., 1995; Rozovskaya et al., 1984; Rudd et al., 1994; Sosunov et al., 2003), but endopyrophosphorolysis reactions are also known (Rudd et al., 1994; Sosunov et al., 2003). In both exo- and endopyrophosphorolysis, PPi acts as the attacking nucleophile to break the RNA chain releasing a short (poly)nucleotide with a 5'-triphosphate. Although the mechanism is not clearly known, PPi addition suppresses misincorporation by both RNAPs and DNAPs (Kahn and Hearst, 1989; Lecomte et al., 1986; Vaisman et al., 2005). Because the pyrophosphorolysis reaction is launched from the pre-translocated elongation complex, PPi can be used as a probe of the pre-translocated state.

Experimental Procedures

Cell culture, extracts and proteins

HeLa cells were purchased from the National Cell Culture Center (Minneapolis, MN) and were prepared as described (Shapiro et al., 1988). Recombinant human TFIIF was prepared as described (Wang et al., 1993; Wang et al., 1994), while TFIIS was purified by phosphocellulose chromatography followed by MonoS chromatography.

Pyrophosphorolysis

Pyrophosphorolysis reaction was performed to test the ability of sodium PPi to mediate the reverse reaction of RNA synthesis. We utilized a procedure similar to the running start two bond protocol as described (Nedialkov et al.,

2003a; Nedialkov et al., 2003b; Xiong and Burton, 2007; Zhang and Burton, 2004). Adenovirus major late promoter with a modified downstream sequence was utilized to produce a 40-nucleotide transcript ending in 3'-CMP (C40), which can be synthesized in the absence of ATP and GTP. HeLa cells were the source of transcription factors and RNAP II. C40 was synthesized by adding 10 μM dATP, 300 μM ApC dinucleotide, 5 μCi per reaction of [α-^{32}P]CTP and 20 μM UTP. Elongation complexes were then washed with 1% Sarkosyl and 0.5 M KCl to remove loosely bound proteins and transcription factors. The complexes were subsequently equilibrated in transcription buffer containing 16 mM $MgCl_2$, 1 μM CTP and UTP (to maintain C40) with and without 12 pmol TFIIF for 30 minutes. On the bench top, 20 μM ATP (initial working concentration of 10 μM) was added for 30 s, for reactions with TFIIF, and 120 s in the absence of TFIIF. This addition allowed C40 elongation complex to extend to A43, in an RNA sequence of 40-CAAAGG-45. A43 complex was injected into the left sample port of the Kintek Rapid Chemical Quench-Flow (RQF-3) instrument and was mixed with 20 mM PPi (10 mM working concentration), injected from the right sample port for 0-30 s. Reactions were then quenched with 0.5 M EDTA. All reactions here and below were done at 25 °C. Because of precipitation, no $MgCl_2$ was added in buffers with PPi, effectively making the final working $MgCl_2$ concentration 8 mM. After quenching, samples were prepared and loaded on a 14% polyacrylamide gel as described (Nedialkov et al., 2003a). The gels were analyzed using a Amersham Bioscience PhosphorImager and each lane was analyzed independently, by

utilizing ImageQuant 5.2 by Molecular Dynamics, for percent signal present in A41 to determine the activity PPi mediated A43→A41 cleavage.

Elongation reactions

Transcription elongation reactions were done similarly to as described (Nedialkov et al., 2003a), and above. Briefly, utilizing the same modified adenovirus major late promotor as above, we synthesized C40 by adding 10 μM ATP, 300 μM ApC dinucleotide, 5 μCi per reaction of [α-^{32}P]CTP and 20 μM UTP. After washing elongation complexes with 1% Sarkosyl and 0.5 M KCl, complexes were equilibrated with transcription buffer with and without TFIIF depending on the reaction protocol (see individual Figures). For reactions with 10 mM PPi in the ATP pulse solution (Figure 2.2), 4 mM ATP (2 mM initial working concentration) was added with or without 20 mM PPi (10 mM working concentration) for 30 s for samples containing TFIIF, and 60 s for samples without TFIIF to synthesize A43 on the bench top. A43 was injected into the left sample port of the RQF-3 instrument then mixed with chase solution containing 5 mM GTP and CTP (2.5 mM final working concentration) injected from the right sample port for 0-30 s as indicated. For reactions with 10 mM PPi in chase solution (Figure 2.3, Figure 2.7 and Figure 2.8*A*), 20 μM ATP (10 μM initial working concentration) was added to C40 for 30 s to synthesize A43 on the bench top and was injected into the left sample port of the RQF-3. Then chase solution containing 200 μM or 5 mM (100 μM or 2.5 mM working concentration respectively) substrate GTP and CTP (also UTP in Figure 2.8) with and without

20 mM PPi, 20 mM phosphate or 40 mM phosphate (10 mM, 10 mM and 20 mM working concentrations respectively) was injected in the right sample port and mixed with A43 for 0-30 s. Reactions with TFIIS (Figure 2.5 and Figure 2.6) were done essentially identically to samples with 10 mM PPi in the ATP pulse solution (see above), except 3 pmol TFIIS was added either with chase (Figure 2.5) or with ATP pulse (Figure 2.6). Upon completion, all reactions were quenched with 0.5 M EDTA and were handled and analyzed as described above. Individual bands were analyzed independently for percent A41 through A43 to determine pause suppression at a stall (A43) when A41 cleavage products were present, while percent A43 was used to determine pause suppression properties when A41 cleavage products were minimal. Percent A41 or U38 was used to determine TFIIS cleavage properties while percent G44 plus all longer products were used to study the initial burst. All reactions were done at 25 °C.

Misincorporation studies

In order to study the effectiveness of PPi to inhibit misincorporation, the same general protocol and template sequence for RNA synthesis was utilized. After generating C40 elongation complex in the presence of TFIIF, A43 was synthesized by adding 20 μM ATP pulse (10 μM working concentration) for 30 seconds. Then chase of 2 mM NTP (1 mM working) with and without PPi was added. NTPs used include GTP, ATP, 3'-dGTP, dGTP, dATP, dTTP, dCTP and CTP. Upon completion, all reactions were quenched with 0.5 M EDTA and were dried down, soaked in loading buffer and boiled. After boiling, all samples were

separated on a 14% polyacrylamide gel and were analyzed as described above. Samples with GTP and ATP chase were quantitated as volume percent above A43 (44^{th} position and beyond). These numbers (see Figure 2.4 numbers within circles) were used to study the percentage of elongation complex that was able to incorporate a correct or incorrect substrate and translocate beyond the 43^{rd} stall position.

Analog studies

To study the effects of UTP analogs on the disappearance of C46, we utilized the same protocol as above to generate C40 elongation complex in the presence of TFIIF. After synthesizing A43, by incubating the reaction with 20 μM ATP pulse (10 μM working concentration) for 30 s, chase solution of 20 mM PPi (10 mM working concentration), 200 μM GTP, 200 μM CTP with and without 200 μM analogs (100 μM working concentration) were added on the bench top for 30 s. These reactions were quenched with 0.5 M EDTA following the chase incubation on the bench top. Samples were handled, separated on a 14% polyacrylamide gel and analyzed as described above.

Results

PPi stimulates 3'-dinucleotide cleavage of a nascent RNA

Mixing PPi with RNAP II elongation complexes has been shown to stimulate pyrophosphorolysis and endopyrophosphorolysis. Pyrophosphorolysis is the reversal of the forward elongation reaction and releases a mononucleotide

triphosphate from the 3'-end of the RNA chain, shortening the RNA by one nucleotide (Chafin et al., 1995; Rozovskaya et al., 1984; Rudd et al., 1994; Sosunov et al., 2003). On the other hand, PPi acting on an arrested elongation complex results in cleaving the RNA chain internally (Rudd et al., 1994; Sosunov et al., 2003). As in pyrophosphorolysis, PPi acts as the attacking nucleophile in the endopyrophosphorolysis reaction, releasing a short RNA fragment with a 5'-triphosphate. PPi was shown to cleave a Drosophila RNAP II elongation complex in dinucleotide increments, producing the same nascent RNA products as were produced by the reaction stimulated by TFIIS (Chafin et al., 1995). Based on analysis using high performance liquid chromatography, released RNA products were interpreted as NTPs, although some of these short RNAs may have been pppNpN products (N=any nucleotide) produced by endopyrophosphorolysis that failed to resolve from pppN markers.

In Figure 2.1, we show that PPi stimulates cleavage of Hs RNAP II A43 elongation complexes (a 43-nucleotide RNA ending in 3'-AMP) primarily in a dinucleotide increment (A43→A41). PPi-mediated cleavage products align with TFIIS-mediated cleavage products on a gel (data not shown). Little or no indication of mononucleotide cleavage (A43→A42) can be detected, indicating that dinucleotide cleavage by endopyrophosphorolysis is likely to be more prevalent than mononucleotide cleavage by pyrophosphorolysis from the A43 position. PPi-dependent A43→A41 dinucleotide cleavage is stimulated by TFIIF (compare Figure 2.1A to Figure 2.1B), reinforcing the idea that the reaction that we observe is intrinsic to the RNAP II elongation complex.

Figure 2.1 **PPi induces cleavage of a dinucleotide.** The RNA sequence is shown at the top of the figure. Reaction protocols utilizing a KinTek RQF-3 instrument (see Experimental Procedures) are shown above gel images A and B. PPi was added as indicated. Reaction times are in seconds. 0* indicates that ATP pulse and PPi chase were not added to C40 elongation complexes. 0 indicates that ATP was added to C40, but the reaction was stopped by addition of EDTA prior to any further incubation or additions. A) Reactions in the presence of TFIIF (F) with and without PPi. B) Reactions in the absence of TFIIF with and without PPi. C) Phosphorimager quantification at Δt=30 seconds. The -F-PPi experiment was done once (n=1); -F+PPi, +F-PPi and +F+PPi were done three times (n=3).

1 4041 43

ACUCUCUUCCCCUUCUCUUUCCUUCUCUUCCCUCUCCUCCAAAGGCCUUU

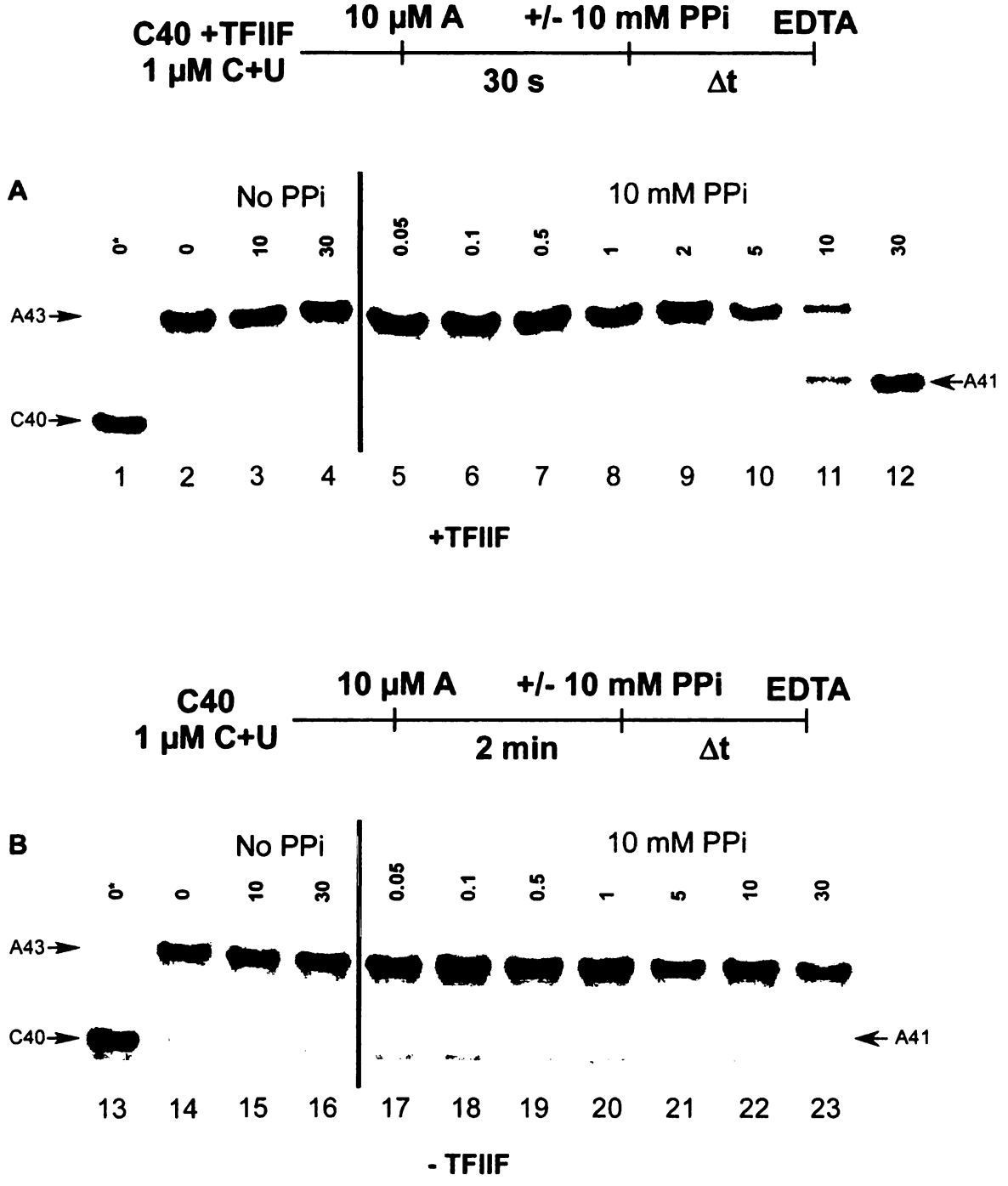

Figure 2.1

Figure 2.1 (cont'd).

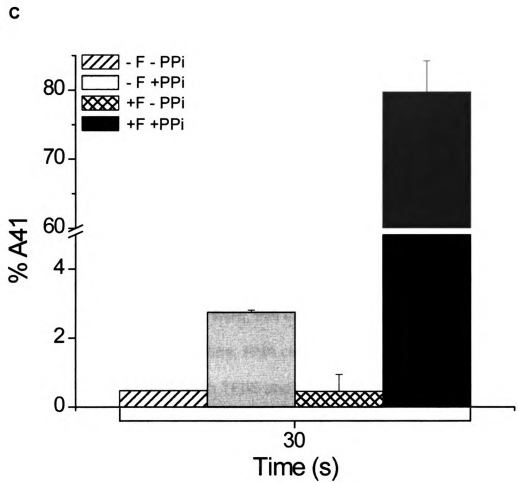

In the absence of TFIIF or the absence of PPi, little or no A43→A41 RNA cleavage is observed (Figure 2.1C). Because TFIIF stimulates A43→A41 endopyrophosphorolysis, 10 mM PPi does not dissociate TFIIF from the elongation complex.

Effects of TFIIF and PPi on elongation and pausing

In Figure 2.2, we tested the effects of TFIIF and PPi on the Hs RNAP II elongation reaction through the sequence 40-CAAAGGCCUUU-50. We find that TFIIF and PPi have multiple effects. First, TFIIF appears to stimulate and PPi appears to suppress misincorporation of AMP for GMP at the 44 position. Second, PPi inhibits elongation very weakly at high NTP concentrations and very strongly at low NTP concentrations. Third, PPi stimulates C40→U38 dinucleotide RNA cleavage, and, at the C40 position, RNA cleavage is reduced in the presence of TFIIF. Furthermore, both TFIIF and PPi suppress pausing by RNAP II.

In Figure 2.2A (first two gels), TFIIF was added to RNAP II elongation complexes that were then extended from the C40 position. In the absence of GTP, addition of 2 mM ATP to C40 is expected to stall the elongation complex at A43. In the presence of TFIIF and the absence of PPi, however, a band is visible at the 44 position prior to GTP addition (compare lanes 2, 14, 26, and 39). This band might be interpreted as misincorporation of AMP from ATP for GMP at the 44 position.

Figure 2.2 **TFIIF and PPi suppress transcriptional pausing. TFIIF stimulates and PPi suppresses mis-incorporation.** A) Gel data. TFIIF and PPi were added as indicated. The RNA sequence is the same as shown in Figure 2.1. 2.5 mM GTP and CTP (G/C) were added where indicated. 0.25 μM UTP is present during the chase because of prior addition. A*44 indicates A44 for G44 mis-incorporation and *, ** indicates elongation of the mis-incorporated A*44 product. 0* indicates that ATP/PPi pulse and GTP/CTP chase were not added to C40; 0 indicates that the ATP/PPi pulse was added but the chase was not. B) Phosphorimager quantification of gels comparing results obtained +/- PPi in the absence of TFIIF. C) Quantification of gels comparing results +/- PPi in the presence of TFIIF. D) Quantification of gels comparing results +/- TFIIF in the absence of PPi. E) Quantification of gels comparing results +/- TFIIF in the presence of PPi. Quantification was expressed as % A43 (percent of total elongation complexes at A43) to show rates of elongation from A43.

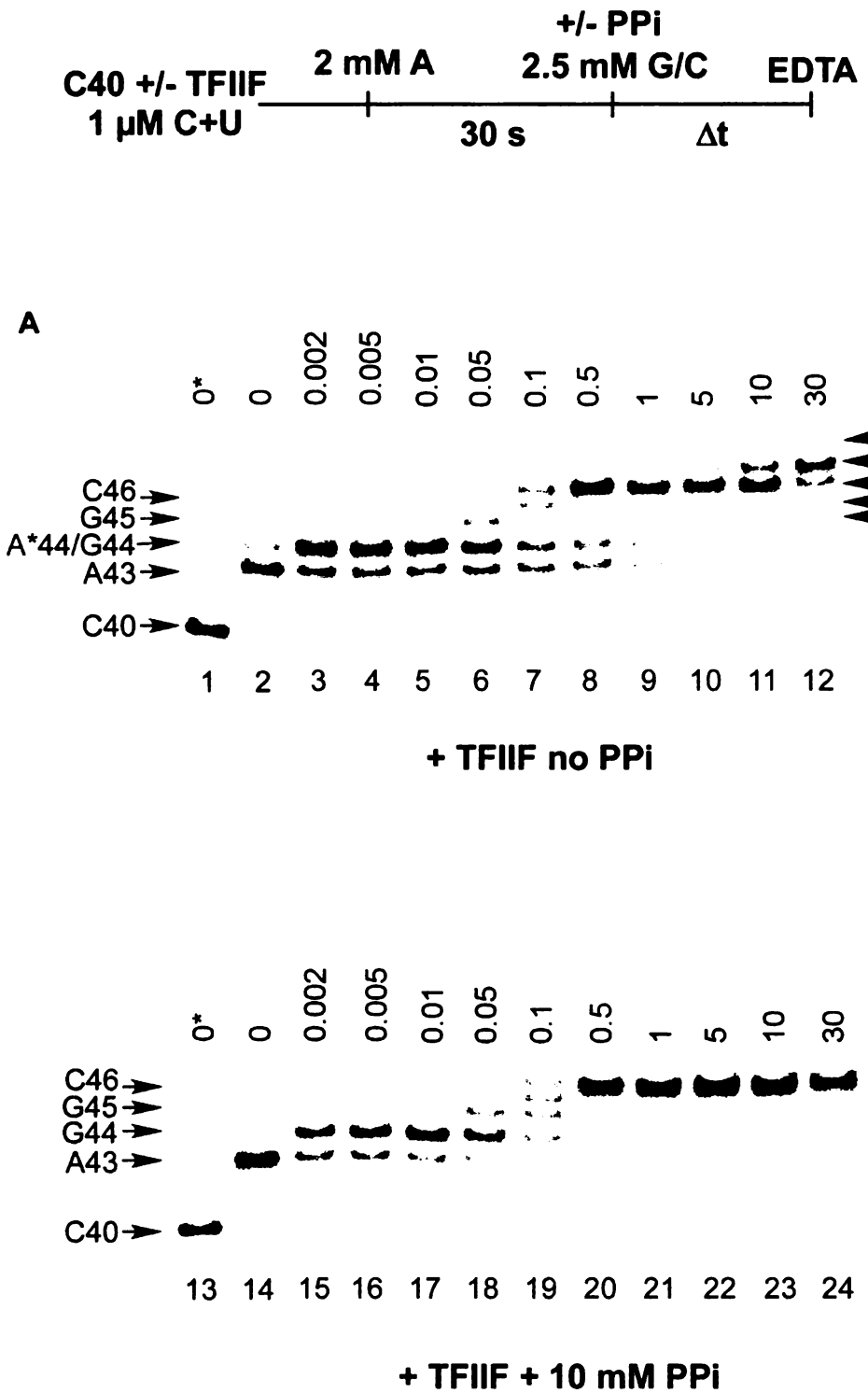
+/- PPi
C40 +/- TFIIF
1 μM C+U
2 mM A
2.5 mM G/C
EDTA
30 s
Δt
A
0*
0
0.002
0.005
0.01
0.05
0.1
0.5
1
5
10
30
U49
U48
C47
**
*
C46
G45
A*44/G44
A43
C40
1 2 3 4 5 6 7 8 9 10 11 12
+ TFIIF no PPi
0*
0
0.002
0.005
0.01
0.05
0.1
0.5
1
5
10
30
C47
C46
G45
G44
A43
C40
13 14 15 16 17 18 19 20 21 22 23 24
+ TFIIF + 10 mM PPi

Figure 2.2

Figure 2.2 (cont'd).

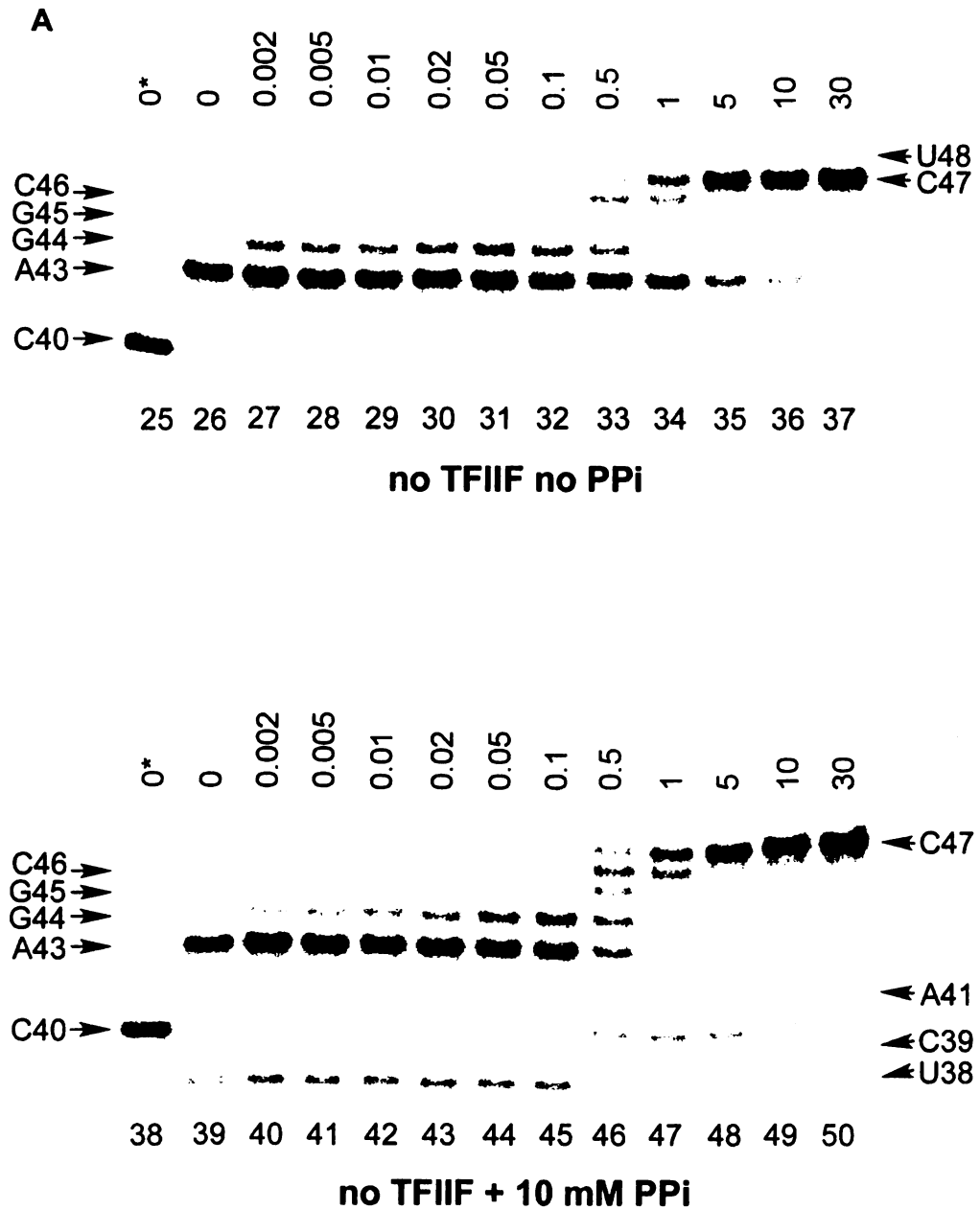

Figure 2.2 (cont'd).

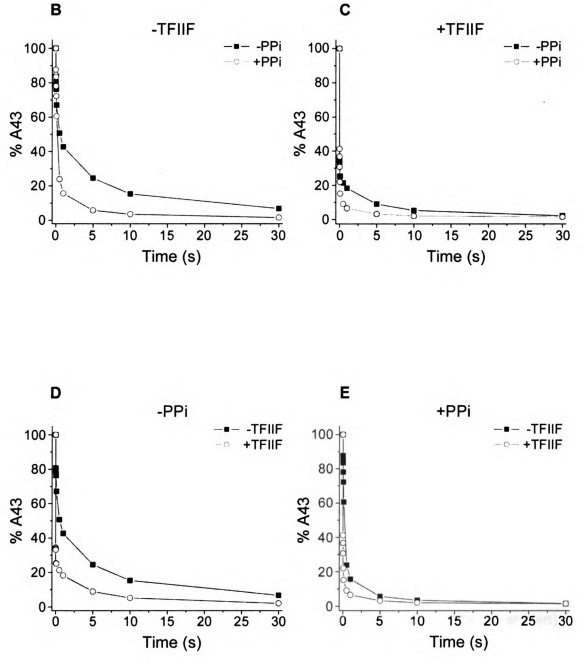

Alternatively, this band might result from scavenging of trace amounts of GTP contaminating other reagents in the assay. However, when GTP and CTP were added, a population of slower elongation complexes was observed advancing from the A*44/G44 position (compare lanes 8-12 to lanes 20-24; note bands marked with * and **; A*44 designates the AMP for GMP misincorporation product). The reduced elongation rate is indicative of slowed extension of the A*44 mismatch, which arises from misincorporation. We suggest, therefore, that TFIIF stimulates and PPi suppresses misincorporation of AMP for GMP at the 44 position (see below).

At 2.5 mM GTP and CTP, little PPi inhibition of elongation is observed through the G44, G45, C46, and C47 positions (compare lanes 6 and 7 with lanes 18 and 19 and lanes 33 and 34 with lanes 46 and 47). At 0.25 μM UTP, by dramatic contrast, PPi all but eliminates detection of U48 (compare lanes 10-12 with lanes 22-24). In the absence of TFIIF, little U48 is detected, whether or not PPi is added, showing that TFIIF promotes incorporation of trace NTP substrates, an effect that is reversed in the presence of PPi. We conclude that TFIIF stimulates and PPi suppresses incorporation of trace NTPs, but that the inhibitory effects of PPi are largely overwhelmed at higher NTP concentrations. These results are not unique to the template positions shown (data not shown). Because TFIIF stimulates elongation in the presence of PPi, 10 mM PPi does not dissociate TFIIF from the elongation complex.

As in Figure 2.1, a dinucleotide RNA cleavage reaction is observed in Figure 2.2. A43→A41 RNA cleavage is weakly detected (lanes 48-50), but,

because 2 mM ATP is present, A41 cleavage products are expected to rapidly extend to A43. In Figure 2.1, 10 μM ATP was added, which was insufficient for efficient extension from A41 to A43 once PPi was added. In the presence of PPi, C40→U38 RNA cleavage is apparent (lanes 14-18 and lanes 39-47). C40→C39 mononucleotide RNA cleavage may also occur, as expected from the exopyrophosphorolysis reaction. From the C40 position, RNA cleavage reactions are more apparent in the absence of TFIIF than in its presence, indicating that the effects of TFIIF on pyrophosphorolysis and endopyrophosphorolysis at different template positions may be complex.

TFIIF has been shown to suppress transcriptional pausing (Bengal et al., 1991; Izban and Luse, 1992; Lei et al., 1999; Renner et al., 2001; Tan et al., 1994). We were surprised, however, to discover that 10 mM PPi appeared to have a similar effect on stalled A43 elongation complexes (compare lanes 9-12 with lanes 21-24). Using phosphorimager quantification (Figures 2.2B-2.2E), we compare transcriptional pausing at the A43 position in the presence and absence of TFIIF and PPi. We find that both TFIIF and PPi suppress pausing. PPi suppresses pausing in the absence or presence of TFIIF (compare Figures 2.2B and 2.2C). As expected, TFIIF suppresses pausing in the absence of PPi (Figure 2.2D). PPi is almost as effective as TFIIF in suppressing pausing (Figure 2.2E).

In Figure 2.3, the timing of PPi addition to the reaction was changed relative to Figure 2.2. In this case, PPi was added at the same time as 2.5 mM GTP and CTP. 10 μM ATP was sufficient for A43 synthesis because PPi was not present during the ATP pulse.

Figure 2.3 **PPi inhibits elongation strongly at low NTP concentrations but not at high NTP concentrations.** The RNA sequence and protocol are shown at the top of the figure. The experiment is similar to that shown in Figure 2.2, except that the order of some additions and the concentration of ATP were different. A) Gel data. 2.5 mM GTP and CTP were added to advance the elongation complex from A43. 0* indicates the ATP pulse and GTP/CTP/PPi chase were not added to C40; 0 indicates that the 10 μM ATP pulse was added, but the chase was not added. B) Phosphorimager quantification of the gel images shown in A, using 1 and 30 second time scales. Quantification was expressed as A41 plus A43 (% of total elongation complexes) versus time. A41 was included in quantification to account for A43 to A41 endopyrophosphorolysis (Figure 2.1).

1 40 43

ACUCUCUUCCCCUUCUCUUUCCUUCUCUUCCCUCUCCUCCAAAGGCCUUU

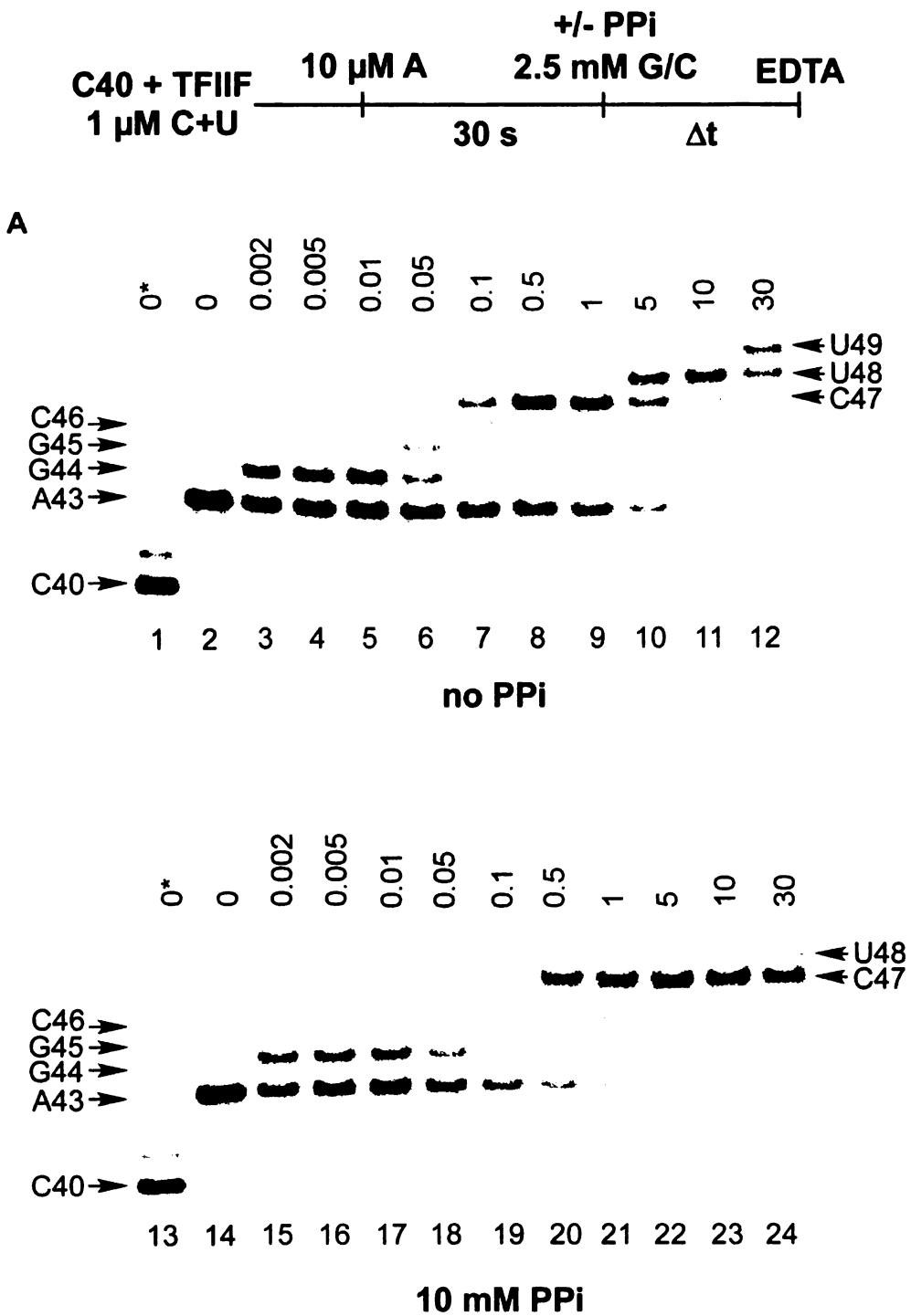

Figure 2.3

Figure 2.3 (cont'd).

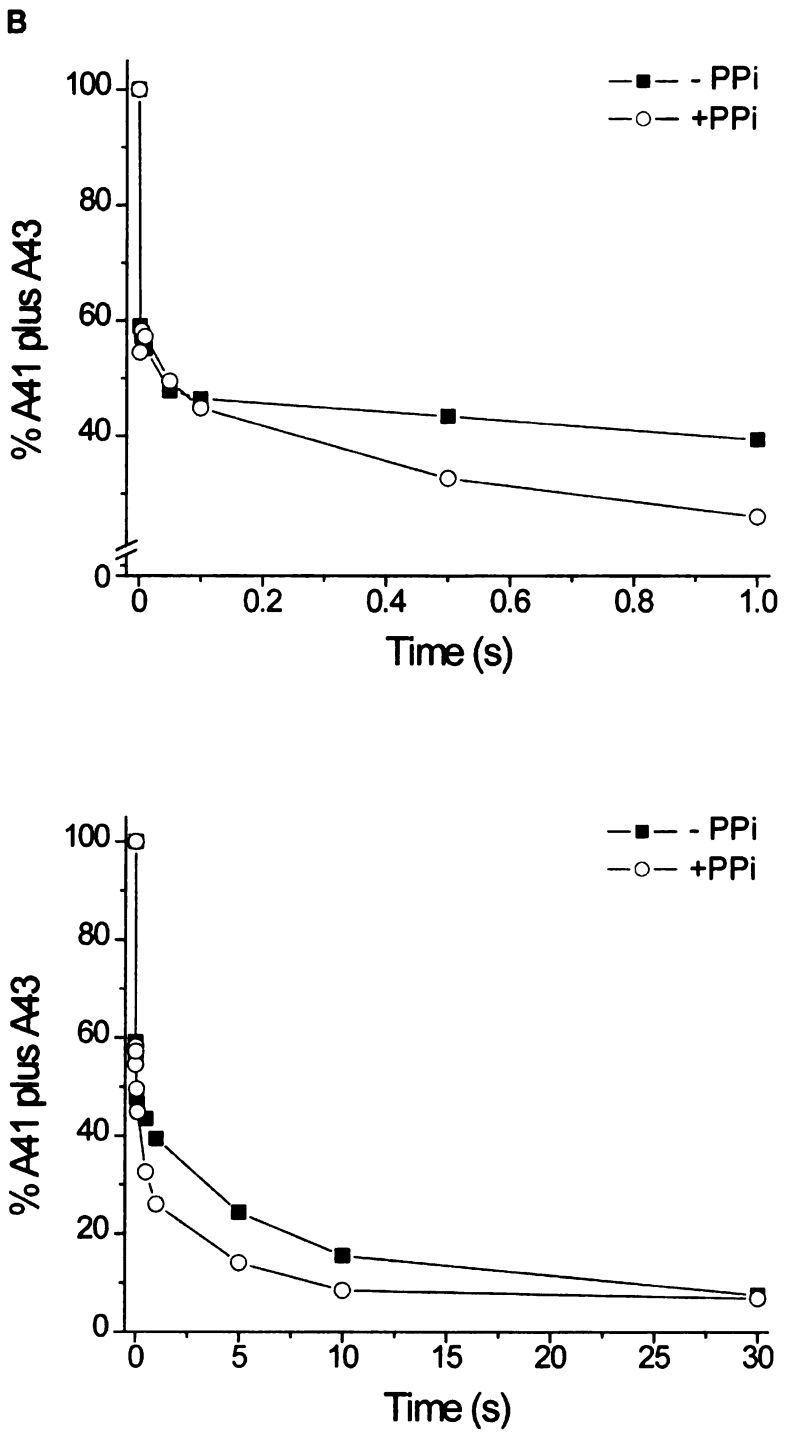

Misincorporation of AMP for GMP at the 44 position is less apparent than in Figure 2.2A because of the reduced ATP concentration (Figure 2.3A). PPi suppresses U48 synthesis (Figure 2.3A). Even when added with elongation substrates, PPi suppresses transcriptional pausing at A43 (Figure 2.3B), indicating that PPi may interact with paused A43 elongation complexes to convert them back onto the active synthesis pathway. If PPi can only trap elongation complexes on the active synthesis pathway once they have re-entered, PPi must be much more potent than accurately templated NTP substrates in preventing pausing re-entry. Otherwise, PPi could not strongly suppress pausing when added at the same time as NTP substrates, compared to the addition of NTP substrates alone. It appears that PPi can actively release RNAP II from the pausing pathway at A43 but that GTP, the elongation substrate, cannot.

Effects of PPi on misincorporation and NTP scavenging

Because PPi is considered to be a probe for the pre-translocated state and NTP substrates are considered to be a probe of the post-translocated state of the elongation complex, we tested multiple substrate replacements for GTP at the 44 position (and other positions) in the absence or presence of 10 mM PPi (Figure 2.4). Because TFIIF stimulates misincorporation by RNAP II, TFIIF was included in reactions. 1 mM GTP, templated at the 44 and 45 positions, was added in the reactions shown in lanes 3 and 4.

Figure 2.4 **PPi suppresses incorporation of incorrect NTPs.** Experimental protocol is seen above the gel data where TFIIF and PPi were added where indicated. RNA sequence is the same as shown in Figure 2.1. 1 mM NTP(or dNTP) was added where indicated to A43 in the presence and absence of PPi. 0.25 μM CTP is present during chase because of prior addition. Incorporation of wrong NTP is possible at 44, 45, 48 and 49 positions, AMP for GMP at 44 and 45 or CMP for UMP at 48 and 49 respectively. 0* indicates that 10 μM ATP pulse and NTP +/- PPi chase were not added; 0 indicates that 10 μM ATP pulse was added but chase was not. Quantification of lanes 3-6 comparing misincorporation and extension with GTP or ATP +/- PPi is shown above gel lanes encased within a circle. Quantification was expressed as % G/*44+ (percent of total elongation complexes at 44^{th} position and beyond).

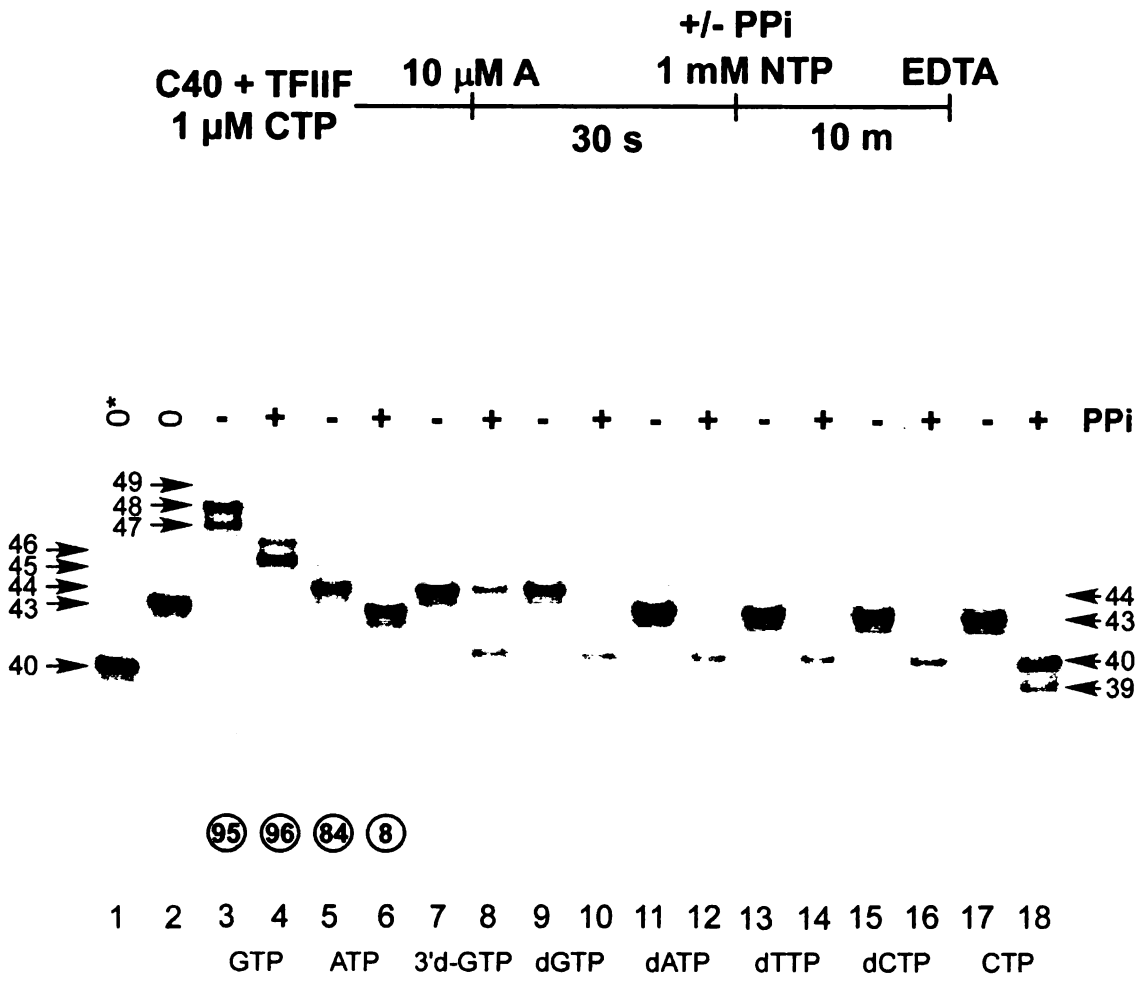
+/- PPi
C40 + TFIIF
1 µM CTP
10 µM A
1 mM NTP
EDTA
30 s
10 m
*O o - + - + - + - + - + - + - + - + PPi
49
48
47
46
45
44
43
40
44
43
40
39
95 96 84 8
1 2 3 4 5 6 7 8 9 10 11 12 13 14 15 16 17 18
GTP
ATP
3'd-GTP
dGTP
dATP
dTTP
dCTP
CTP

Figure 2.4

After 10 minutes in the absence of PPi, the reaction stopped primarily at the C47 and C*48 positions (C*48 indicates that CMP was apparently misincorporated for UMP at the 48 position). The CTP concentration in these reactions is 0.25 μM. In the presence of 10 mM PPi, elongation stops at G45 and C46, indicating that PPi suppresses incorporation of CMP at the C46 and C47 positions at 0.25 μM CTP. In Figure 2.2 (compare lane 2 to lane 14), we showed evidence that PPi might suppress misincorporation of AMP for GMP at the 44 position. In the presence of 1 mM ATP and the absence of PPi (Figure 2.4, lane 5), elongation stops primarily at A*44. Phosphorimager quantification indicates that about 84% of complexes advance from the A43 position, indicating efficient misincorporation of AMP for GMP. Some transcripts appear to stop at the A*A*45, A*A*CC47, and A*A*CCC*48 positions (* indicates likely misincorporation positions at or near the 3'-end of the RNA). When 10 mM PPi is added to the reaction (lane 6), most elongation stops at the A43 position. Only a trace of A*44 is detected (only about 8% of total A43 transcripts advance). PPi appears to strongly suppress misincorporation of AMP for GMP at the 44 template position.

Using the chain terminator 3'-dGTP as substrate, 3'-dGMP is incorporated whether or not PPi is added (lanes 7 and 8). In the presence of PPi, however, 3'-dG44 transcripts are processed back through the A41 position. These transcripts may remove the 3'-dG chain terminator by exopyrophosphorolysis (3'dG44→A43) followed by A43→A41 endopyrophosphorolysis, followed by additional PPi-dependent processing events. Apparently, 3'-dG in the i site (the position of the 3'-end of the RNA in the post-translocated elongation register) and

3'-dGTP in the i+1 NTP substrate site are not sufficient to prevent pyrophosphorolysis, a reaction that requires reversion to the pre-translocated state (3'-dG44 in i+1). A very similar observation is made with 2'-dGTP as substrate (lanes 9 and 10), although in this case further elongation from the 44 position is possible because dGTP is not a chain terminator. In the absence of PPi, small amounts of dGdGCC47 and dGdGCCC*48 are apparent. In lanes 13-20, dATP, dTTP, dCTP, and CTP were also tested for incorporation at the 44 position. In the presence of PPi, transcripts are processed back to the A41 position and to shorter positions. In the presence of dATP and PPi, there is weak evidence of synthesis of dA42 in the presence of PPi, presumably occurring after A43→A41 dinucleotide cleavage (lane 12). In the absence of PPi, there is evidence of misincorporation of AMP for GMP at the 44 position (see lanes 11, 13, and 15). These reactions include 5 μM ATP, because of prior addition for A43 synthesis. It does not appear that dAMP, dTMP, dCMP, or CMP are significantly misincorporated within 10 min incubation at the 44 position, even in the absence of PPi (lanes 11, 13, 15, and 17). To summarize, in the presence of PPi, there is weak evidence of AMP from ATP for GMP misincorporation at the 44 position, and 3'dGMP and dGMP can also be incorporated for GMP at the 44 position. There is no evidence for dAMP, dTMP, dCMP, or CMP misincorporation at the 44 position in the presence or absence of PPi. In the presence of PPi, there is evidence of dAMP incorporation for AMP at the 42 position (lane 14). We conclude that PPi suppresses misincorporation and also suppresses scavenging of limiting NTPs, even when the trace NTP is accurately templated.

Effects of TFIIS

Because PPi suppresses transcriptional pausing, and because the elongation factor TFIIS stimulates RNA cleavage of paused elongation complexes (Fish and Kane, 2002; Gu and Reines, 1995; Rudd et al., 1994), we predicted that addition of PPi might inhibit subsequent RNA dinucleotide cleavage stimulated by TFIIS (Wang and Hawley, 1993). Essentially, TFIIS can be used as a probe for the pausing, RNA cleavage, and re-start pathway, while PPi can be used as a probe for the active synthesis pathway. Our prediction for the interactive effects of TFIIS and PPi was confirmed by the experiment shown in Figure 2.5. 10 mM PPi was added to the reaction 30 seconds before addition of TFIIS. Addition of PPi prior to TFIIS strongly inhibited evidence of A43→A41 dinucleotide cleavage (compare lanes 8-10 with lanes 19-21). In panel B, we show that A43→A41 dinucleotide cleavage is strongly dependent on the presence of TFIIS. Even in the presence of PPi, the A41 product is significantly reduced in amount when TFIIS is absent compared to when TFIIS is present. Therefore, if PPi supports A43→A41 dinucleotide cleavage under these conditions (2 mM ATP in pulse), resulting A41 complexes are rapidly re-extended to A43, minimizing accumulation of A41.

To confirm that PPi suppresses TFIIS-mediated RNA cleavage by retaining RNAP II on the active synthesis pathway (Figure 2.5), PPi was tested for effects on the chemical step of TFIIS-mediated dinucleotide cleavage.

Figure 2.5 **When added prior to TFIIS, PPi appears to inhibit TFIIS mediated A43→A41 dinucleotide cleavage.** The reaction protocol is shown at the top of the figure. A) Gel data. PPi and ATP were added to C40 as indicated. A43→A41 RNA cleavage products are indicated. 0* indicates that ATP/+/-PPi pulse and GTP/CTP chase were not added to the C40 complex; 0 indicates that the pulse was added, but the chase was not. B) Quantification of the gel at the 0.5 and 1 s points. Experiments with -PPi+TFIIS and +PPi+TFIIS were done three times (n=3). The +PPi-TFIIS experiment was done once (n=1) and is included for comparison.

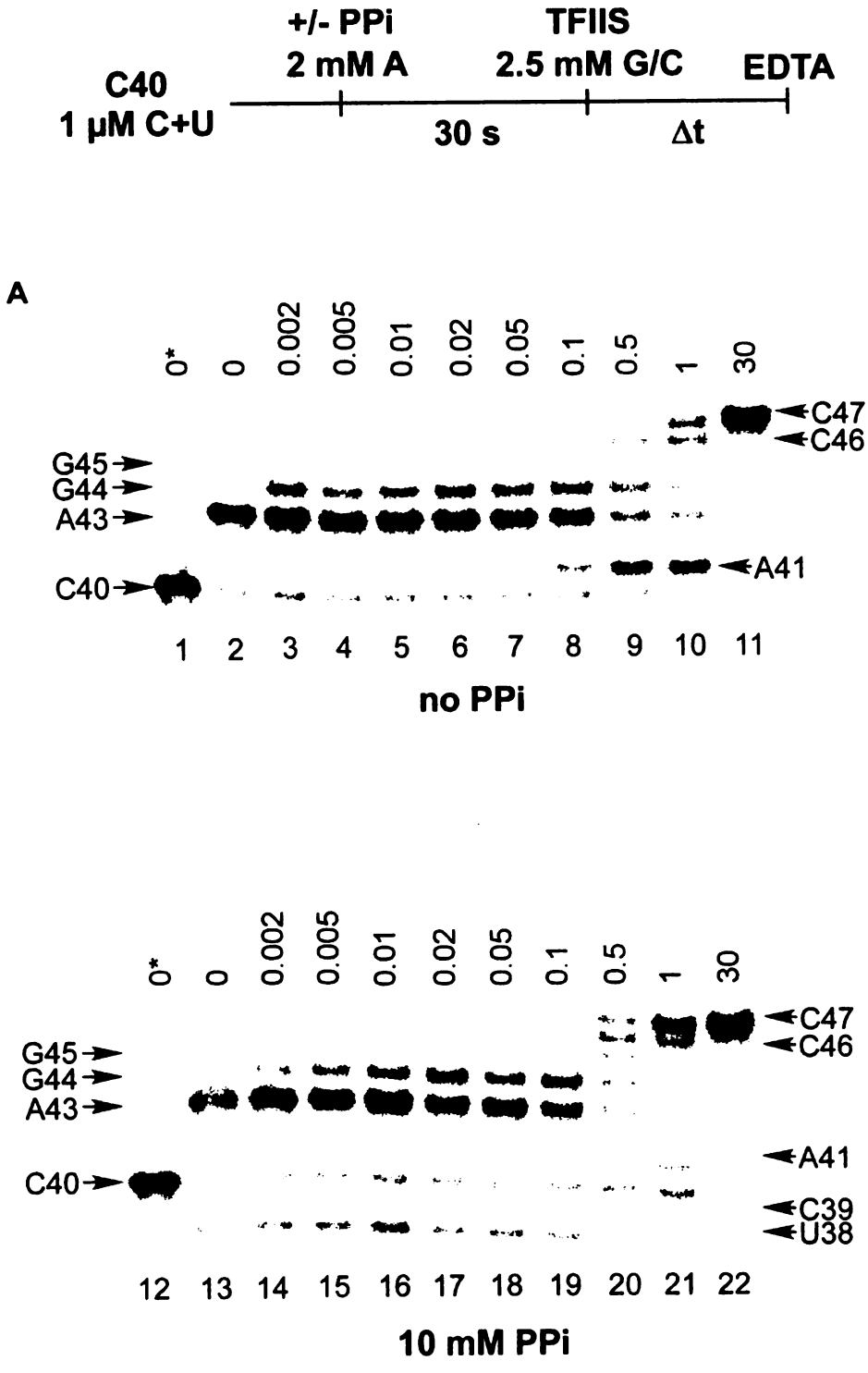
+/- PPi
2 mM A
TFIIS
2.5 mM G/C
EDTA
C40
1 µM C+U
30 s
Δt
A
0*
0
0.002
0.005
0.01
0.02
0.05
0.1
0.5
1
30
C47
C46
G45
G44
A43
A41
C40
1 2 3 4 5 6 7 8 9 10 11
no PPi
0*
0
0.002
0.005
0.01
0.02
0.05
0.1
0.5
1
30
C47
C46
G45
G44
A43
A41
C40
C39
U38
12 13 14 15 16 17 18 19 20 21 22
10 mM PPi

Figure 2.5

Figure 2.5 (cont'd).

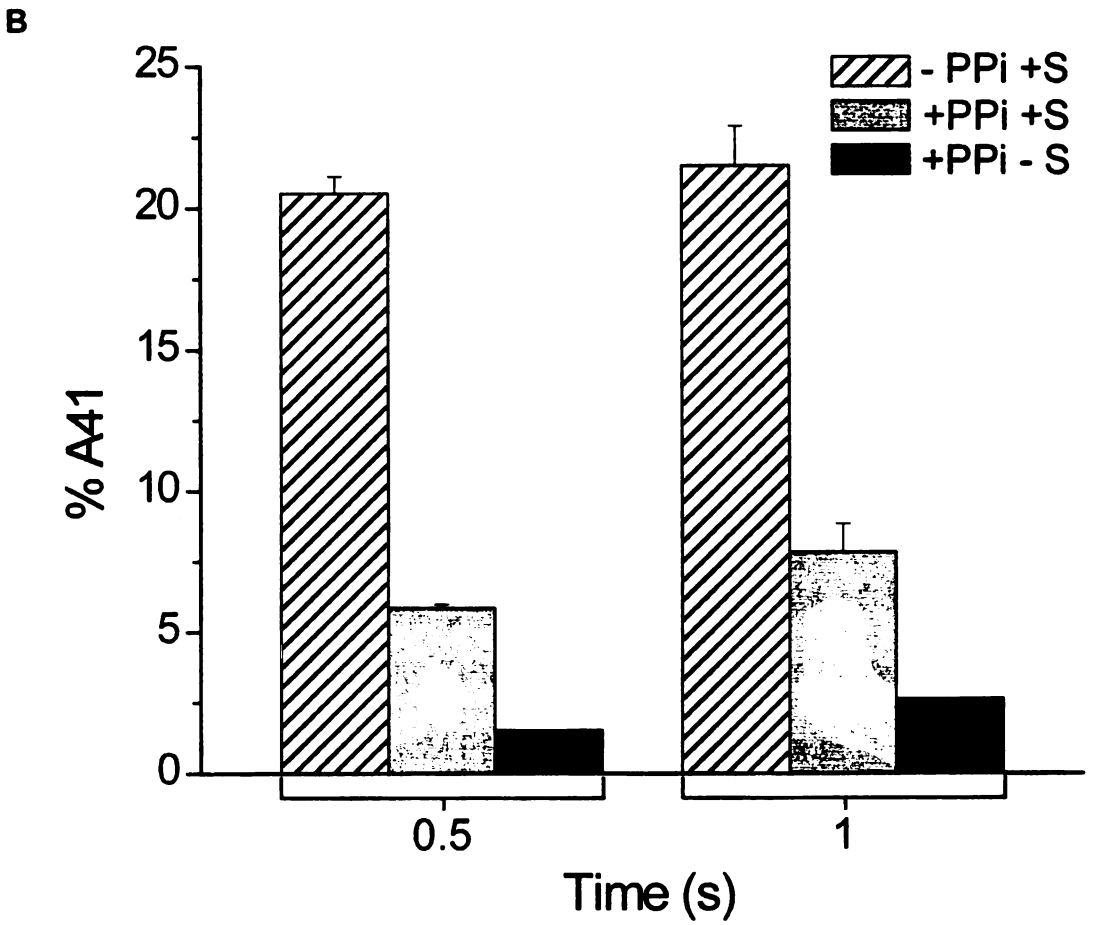

In the experiment shown in Figure 2.6, TFIIS, PPi, and 2 mM ATP were added together, 30 seconds prior to addition of GTP and CTP, to support elongation from the A43 position. In this experimental design, paused C40 elongation complexes were established prior to TFIIS and PPi addition. If C40 elongation complexes are paused, they are expected to be sensitive to TFIIS-mediated cleavage (Fish and Kane, 2002; Gu and Reines, 1995; Rudd et al., 1994). A43 elongation complexes, by contrast, are synthesized only after PPi has been added to the reaction, so, if A43 elongation complexes pause, pausing must occur in the presence of PPi, and PPi blocks pausing.

As we expected, TFIIS-mediated C40→U38 dinucleotide cleavage was not noticeably inhibited by 10 mM PPi addition. Because, in this case, paused and/or backtracked C40 conformations were established prior to addition of PPi, addition of TFIIS resulted in C40→U38 cleavage. By contrast, A43→A41 (compare lanes 2-10 to lanes 15 to 23) and U38→C36→C34→C32 (compare lanes 2 to 15 with lanes 15 to 26) TFIIS-mediated dinucleotide cleavages were inhibited in the presence of 10 mM PPi. Most likely, addition of PPi prior to transcriptional stalling at A43 or prior to RNA cleavage to U38, C36, C34, and C32 allows PPi binding to occur before forming the paused and/or backtracked conformation of the elongation complex that is sensitive to TFIIS cleavage. PPi does not appear to affect the chemical step in TFIIS-mediated dinucleotide cleavage, because, once the paused conformation of the C40 complex forms, PPi no longer influences the C40→U38 dinucleotide cleavage reaction.

Figure 2.6 **When added together, PPi does not inhibit TFIIS mediated dinucleotide cleavage.** A) Gel data. PPi, TFIIS, and 2 mM ATP were added to C40 elongation complexes as indicated. Dinucleotide cleavage products resulting from TFIIS-mediated dinucleotide cleavage from C40 are labeled U38, C36, C34 and C32 respectively. 0* indicates that the ATP/PPi/TFIIS pulse and GTP/CTP chase were not added to C40; 0 indicates that the pulse was added to C40, but the chase was not. B) Phosphoimager quantification at 0 and 0.02 s time points. All dinucleotide cleavage products derived from C40 were totaled as C27 to U38 (% of total transcripts). C) Quantification of dinucleotide cleavage products cleaved from the U38 position. D) C40→U38 dinucleotide cleavage is mostly attributable to TFIIS and not PPi. +PPi-F-S was done 5 times (n=5); +PPi+F-S and +PPi-F+S were done 4 times (n=4).

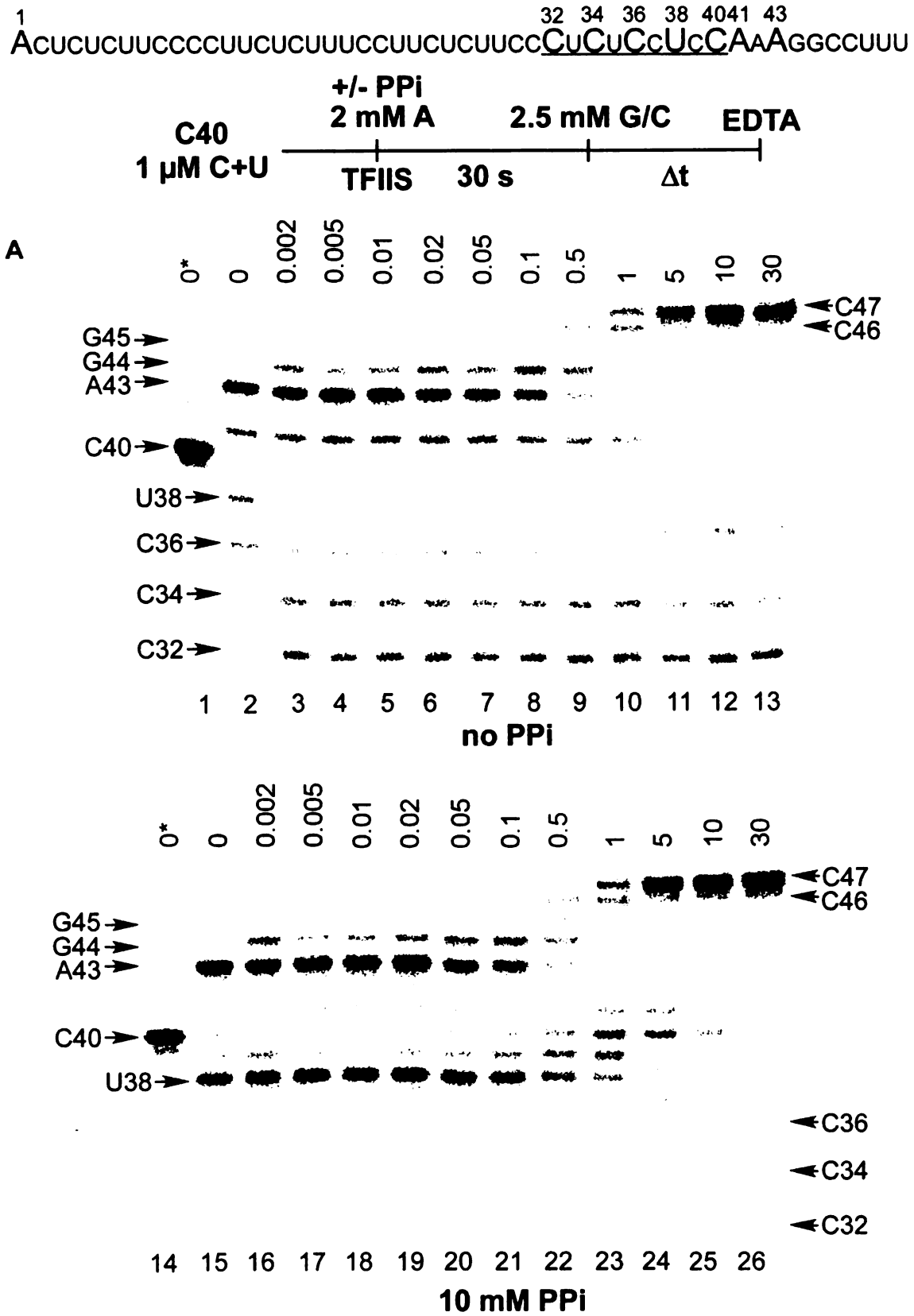
1
ACUCUCUUCCCCUUCUCUUUCCUUCUCUUCCCUCUCCUCCUCAAAGGCCUUU
32 34 36 38 4041 43
+/- PPi
2 mM A
2.5 mM G/C
EDTA
C40
1 µM C+U
TFIIS
30 s
Δt
A
0* 0 0.002 0.005 0.01 0.02 0.05 0.1 0.5 1 5 10 30
C47
C46
G45
G44
A43
C40
U38
C36
C34
C32
1 2 3 4 5 6 7 8 9 10 11 12 13
no PPi
0* 0 0.002 0.005 0.01 0.02 0.05 0.1 0.5 1 5 10 30
C47
C46
G45
G44
A43
C40
U38
C36
C34
C32
14 15 16 17 18 19 20 21 22 23 24 25 26
10 mM PPi

Figure 2.6

Figure 2.6 (cont'd).

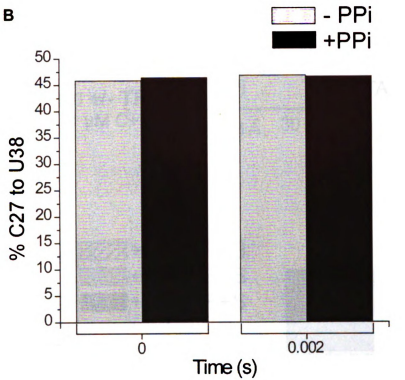

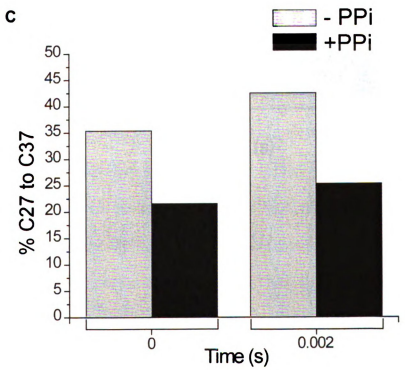

Figure 2.6 (cont'd).

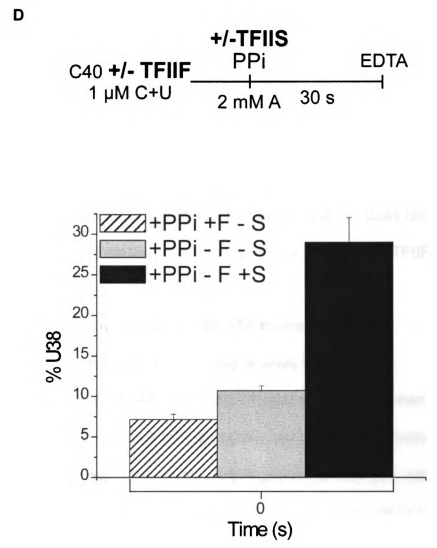

Analyzing these effects using phosphorimager quantification, Figure 2.6B indicates that the sum of C27 to U38 elongation complexes (including all dinucleotide cleavage products from C40) is approximately the same whether or not PPi was added. Figure 2.6C shows that PPi inhibits U38→C36 dinucleotide cleavage, although it does not inhibit C40→U38 cleavage. Figure 2.6D indicates that most C40→U38 dinucleotide cleavage is dependent on TFIIS, rather than PPi. Again, we find that TFIIF decreases PPi-dependent dinucleotide cleavage from the C40 position (Figure 2.6D). Based on these results it seems as though PPi can support dinucleotide cleavage at some positions, but PPi does not strongly stimulate C40→U38 cleavage in the absence or presence of TFIIF.

PPi inhibition of transcription at moderate NTP concentrations

Because PPi suppresses elongation very strongly when NTP concentrations are low (i.e. 0.25 μM UTP and CTP) and very weakly when NTP concentrations are high (i.e. 2.5 mM GTP and CTP), we considered whether PPi would inhibit elongation at moderate NTP concentrations (i.e. 100 μM). With GTP and CTP at 100 μM, PPi inhibits elongation, but the most dramatic effect is observed at C46 and C47, as RNAP II approaches a stall at the C47 position (compare Figure 2.7A lanes 3 to 12 and lanes 15 to 24). In the presence of PPi, transcription is expected to stall because UTP for U48 synthesis is limiting (0.25 μM UTP). Inhibition appears specific to PPi because 10 or 20 mM phosphate, for instance, does not show comparable effects (compare lanes 27 to 37 and lanes 40 to 50 to lanes 15 to 24).

Figure 2.7 **PPi strongly inhibits elongation at moderate NTP concentrations.** A) Gel data. PPi or phosphate was added after A43 synthesis as part of the chase as indicated. The A41 band is identified to indicate A43→A41 dinucleotide cleavage stimulated by PPi. 0* indicates that the ATP pulse and GTP/CTP chase were not added to C40; 0 indicates that the pulse was added, but the chase was not. B) phosphorimager quantification at 1 and 30 second time points. A43 and A41 elongation complexes are summed to account for A43→A41 dinucleotide cleavage stimulated by PPi. C) Quantification of U48 and all longer transcripts to show the rate of incorporation of 0.25 μM UTP (n=3).

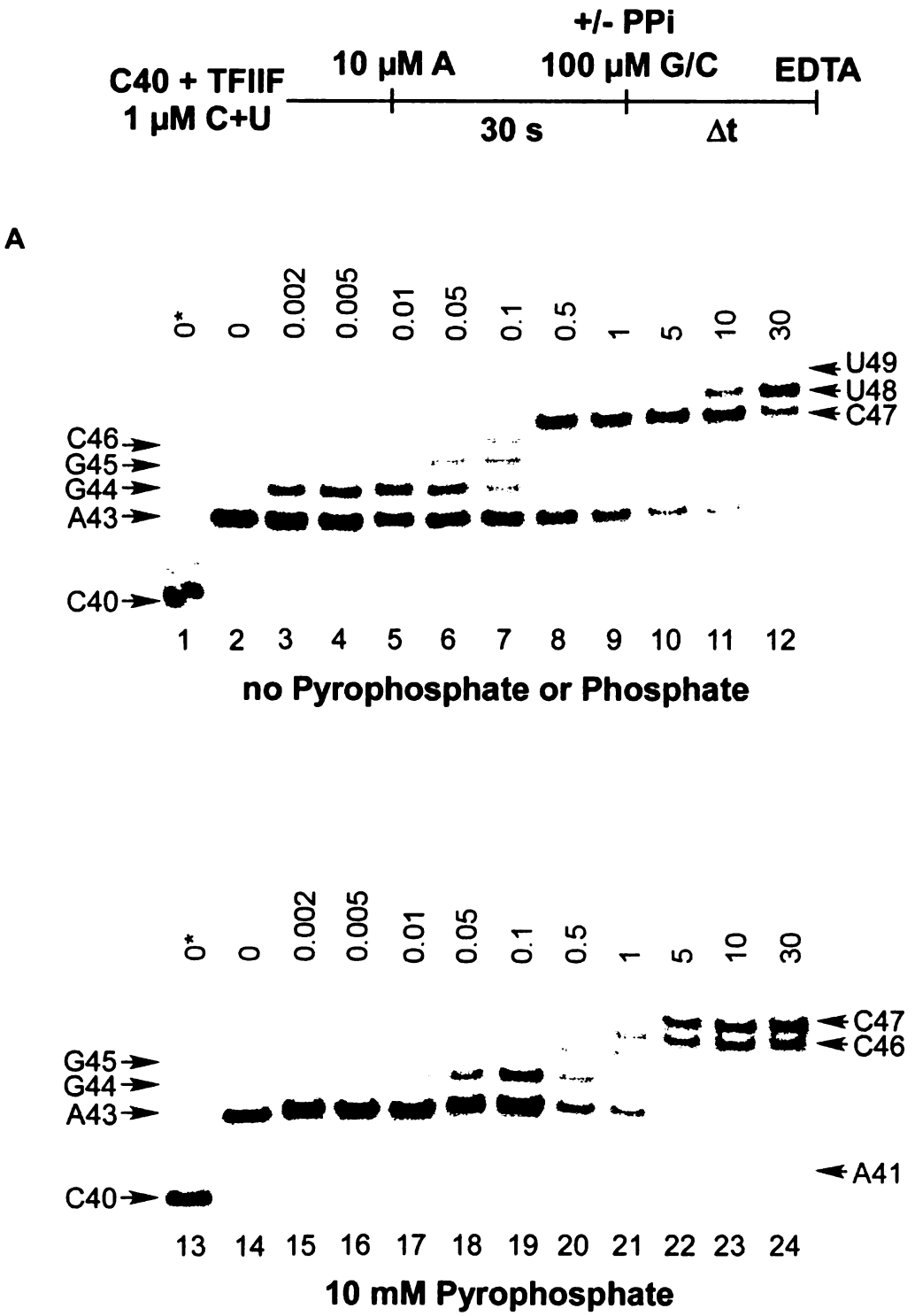
+/- PPi
C40 + TFIIF
1 μM C+U
10 μM A
100 μM G/C
EDTA
30 s
Δt
A
0*
0
0.002
0.005
0.01
0.05
0.1
0.5
1
5
10
30
U49
U48
C47
C46
G45
G44
A43
C40
1 2 3 4 5 6 7 8 9 10 11 12
no Pyrophosphate or Phosphate
0*
0
0.002
0.005
0.01
0.05
0.1
0.5
1
5
10
30
C47
C46
G45
G44
A43
A41
C40
13 14 15 16 17 18 19 20 21 22 23 24
10 mM Pyrophosphate

Figure 2.7

Figure 2.7 (cont'd).

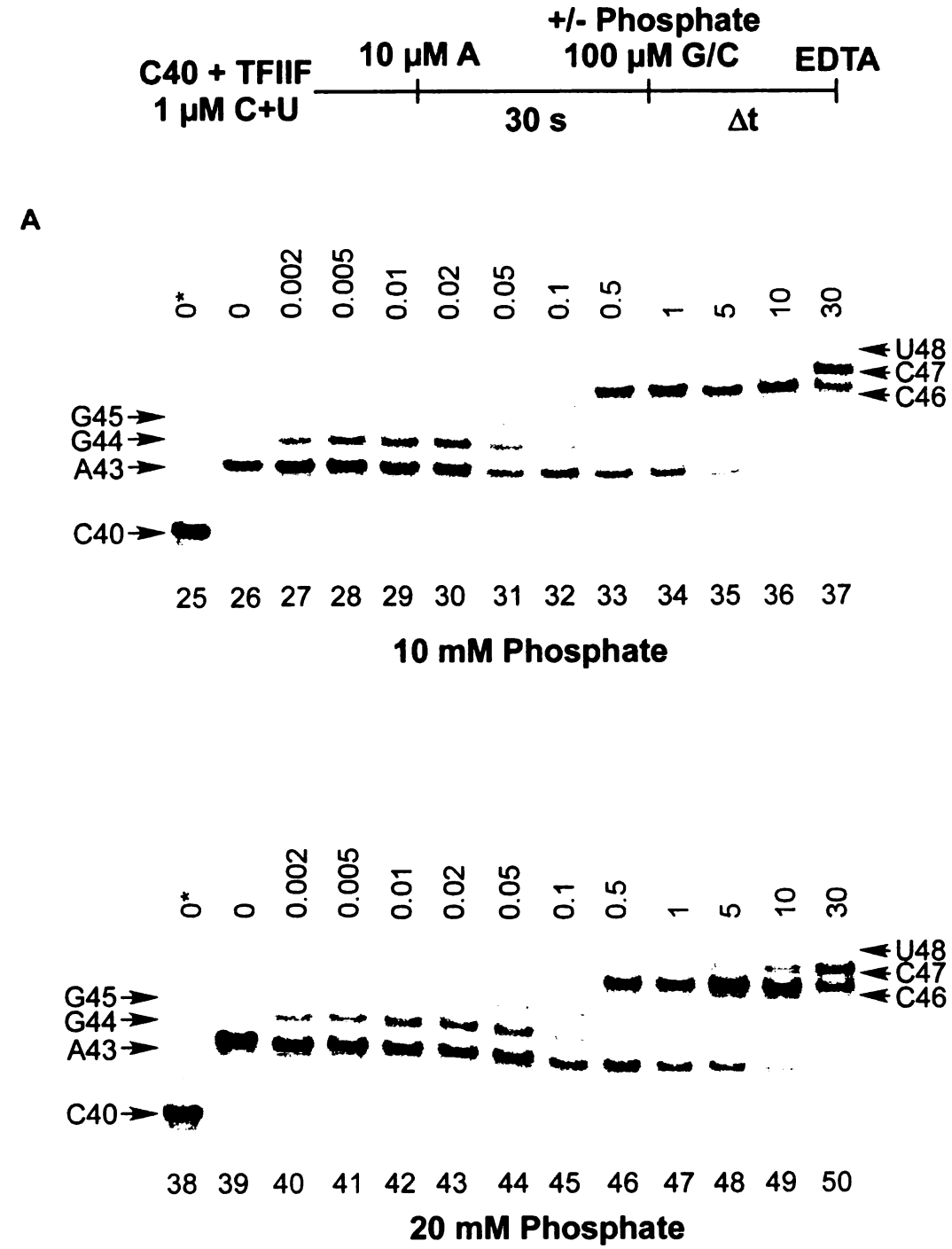

Figure 2.7 (cont'd).

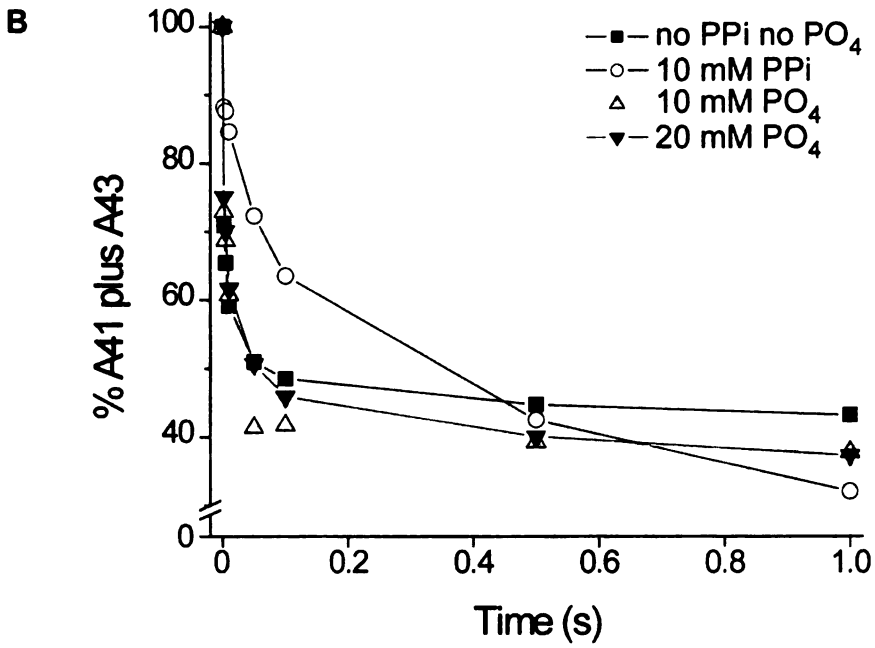

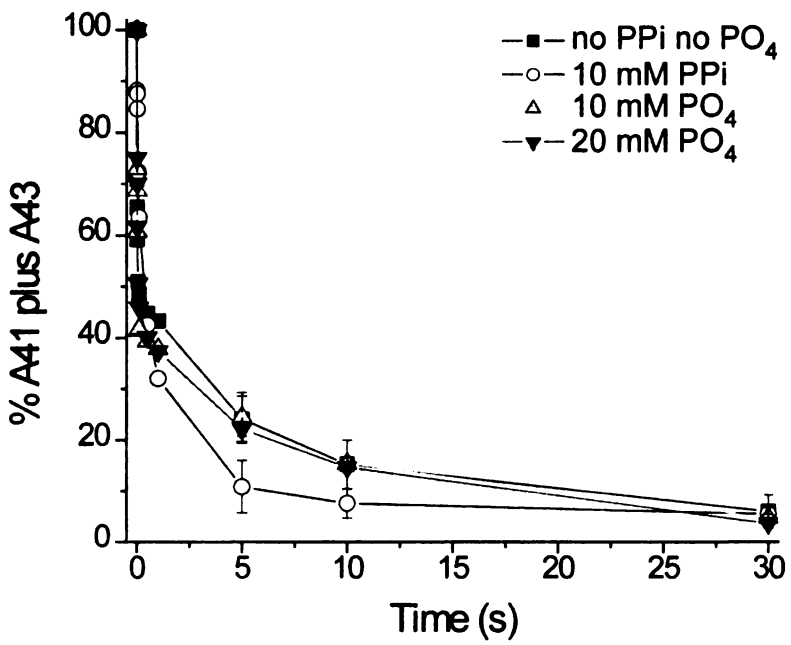

Figure 2.7 (cont'd).

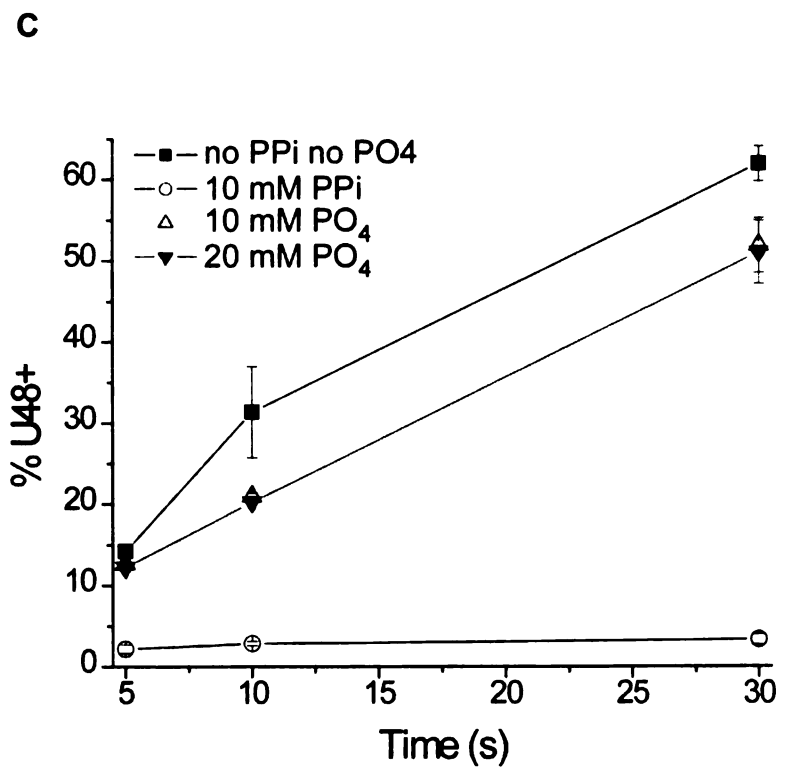

Phosphorimager quantification shows that PPi inhibits elongation (Figure 2.7B, upper panel) and suppresses pausing (Figure 2.7B, lower panel) in ways that phosphate does not. Figure 2.7C shows that PPi suppresses elongation to U48 at 0.25 μM UTP, in a manner that phosphate does not.

To further investigate PPi inhibition of elongation at the C46 and C47 positions (Figure 2.7A lanes 22-24), we considered two possibilities. One possibility was that elongation was arrested at C46. The other possibility, which we considered more likely, was that C46 and C47 approached dynamic equilibrium, such that elongation from C46 to C47 was balanced in rate by pyrophosphorolysis from C47 to C46. This second interpretation was particularly interesting, because potentially, such a balance could be utilized to investigate translocation states of the C46 and C47 elongation complexes.

PPi can be considered to be a probe for the pre-translocated elongation complex, because the pyrophosphorolysis reaction (reversal of chemistry) must be launched from the pre-translocated state (Kashkina et al., 2006; Svetlov et al., 2007). By similar reasoning, NTP substrates must bind to the post-translocated state of the elongation complex to participate in the next bond formation (Abbondanzieri et al., 2005; Bar-Nahum et al., 2005; Kashkina et al., 2006; Vassylyev and Artsimovitch, 2005; Vassylyev et al., 2007; Wang et al., 2006). NTP substrates, therefore, can be considered to be probes for the post-translocated state. We reasoned that a system, in which pyrophosphorolysis was balanced by forward synthesis, should be informative for the dynamic distributions of translocation states at C46 and C47. To be more specific, C46

must exist in the post-translocated state to support C47 synthesis. C47 must exist in the pre-translocated state to support C46 synthesis by pyrophosphorolysis. Addition of UTP tests for the extent of post-translocated C47 complex by allowing elongation to U48.

If C46 is not arrested and can extend to C47, addition of UTP will cause both C46 and C47 to advance (Figure 2.8A) (compare lanes 9-13 with lanes 22-26). C46 elongates to C47 and longer positions in the presence of 100 μM UTP, although the rate of elongation is slow at multiple positions. C46, C47, U48, and U49 bands are visible for many seconds, as if elongation and pyrophosphorolysis might occur simultaneously at each position. In Figure 2.8B, we show that, in the presence of PPi, UTP is required for C46 to advance. As expected, in the absence of PPi, elongation does not halt at C46. 3'-deoxy-UTP, which is a chain-terminating substrate for RNAP II and a close UTP analogue, allows C46 to advance slightly. Though 100 μM GTP and CTP are present in the reaction, ATP, dTTP, UDP, and 2'-deoxy-UTP do not stimulate C46 to advance in 30 seconds. This result shows that UTP, acting as a substrate for U48 synthesis, stimulates C46 elongation. Even the close UTP analogue 3'-deoxy-UTP does not strongly support C46 extension.

To confirm that C46 is formed by pyrophosphorolysis from C47, we did the experiment shown in Figure 2.8C. In this case, the elongation complex was advanced to C47 by addition to A43 complexes of GTP and CTP.

Figure 2.8 **C46 elongation to C47 and C47 pyrophosphorolysis to C46 appear to be at dynamic equilibrium, indicating a mixture of pre- and post-translocated elongation complexes at the C47 stall position.** A) Gel data. 100 μM UTP was added as indicated. 0* indicates ATP pulse and GTP/CTP/UTP/PPi chase were not added to C40; 0 indicates that the pulse was added but not the chase. B) Other NTPs and UTP analogs were added as indicated. Only 3'-dUTP (a chain terminator) can partially substitute for UTP. All reactions with the exception of the sample -PPi were performed 3 times (n=3). C) At the stall position, C46 is generated by C47→C46 pyrophosphorolysis. In this protocol, PPi was added as a chase after forming C47. 0* indicates that no ATP/GTP/CTP pulse and PPi chase were added to C40; 0 indicates that the pulse was added to C40 but not the chase. Lane 2 contains A43 size marker produced by adding 10 μM ATP to C40.

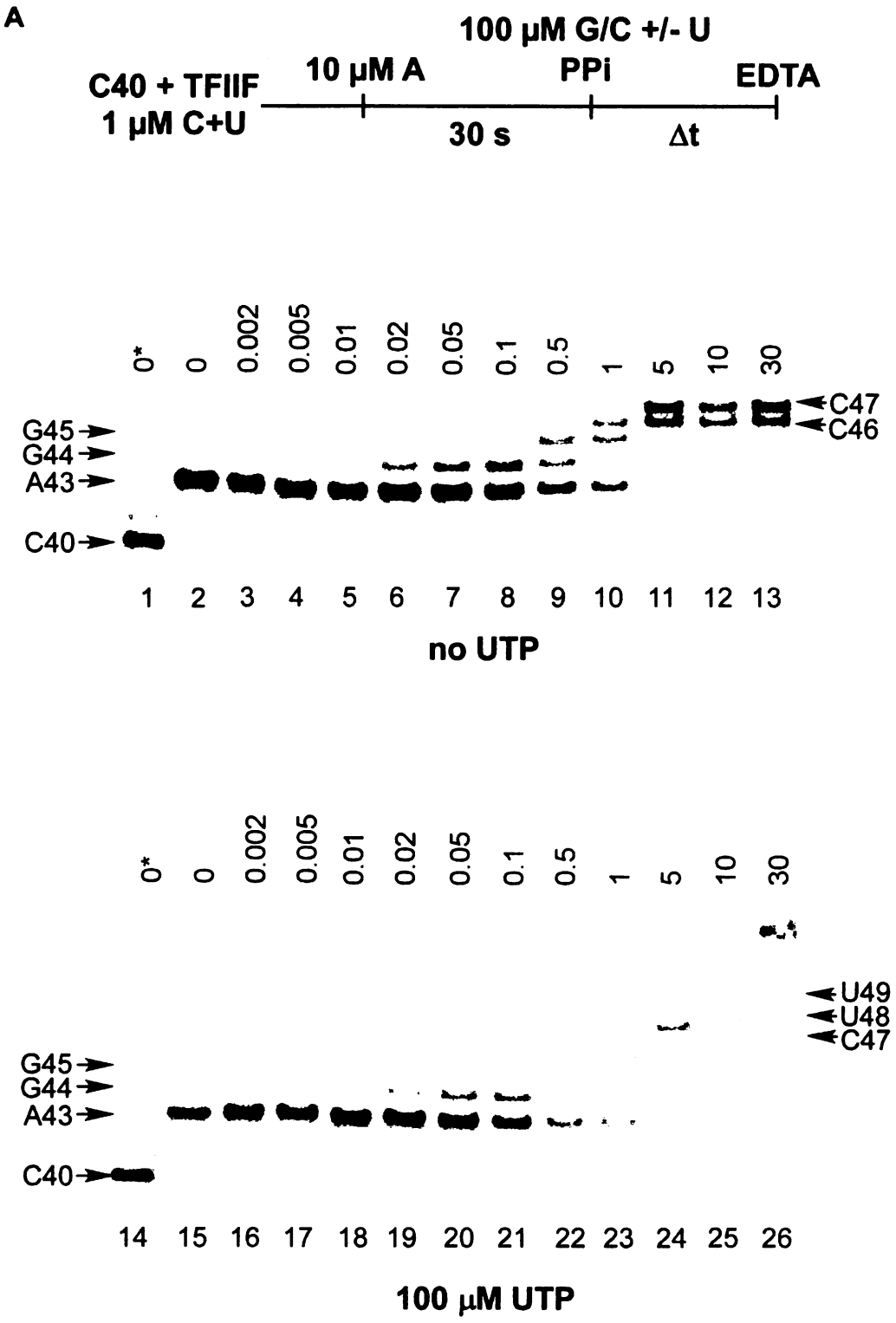
A
100 µM G/C +/- U
C40 + TFIIF
1 µM C+U
10 µM A
PPi
EDTA
30 s
Δt
0*
0
0.002
0.005
0.01
0.02
0.05
0.1
0.5
1
5
10
30
C47
C46
G45
G44
A43
C40
1 2 3 4 5 6 7 8 9 10 11 12 13
no UTP
0*
0
0.002
0.005
0.01
0.02
0.05
0.1
0.5
1
5
10
30
U49
U48
C47
G45
G44
A43
C40
14 15 16 17 18 19 20 21 22 23 24 25 26
100 µM UTP

Figure 2.8

Figure 2.8 (cont'd).

B

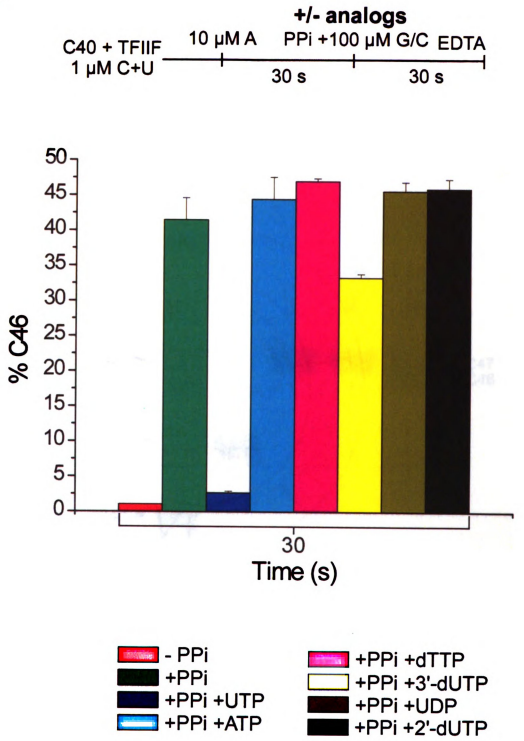

Figure 2.8 (cont'd).

C

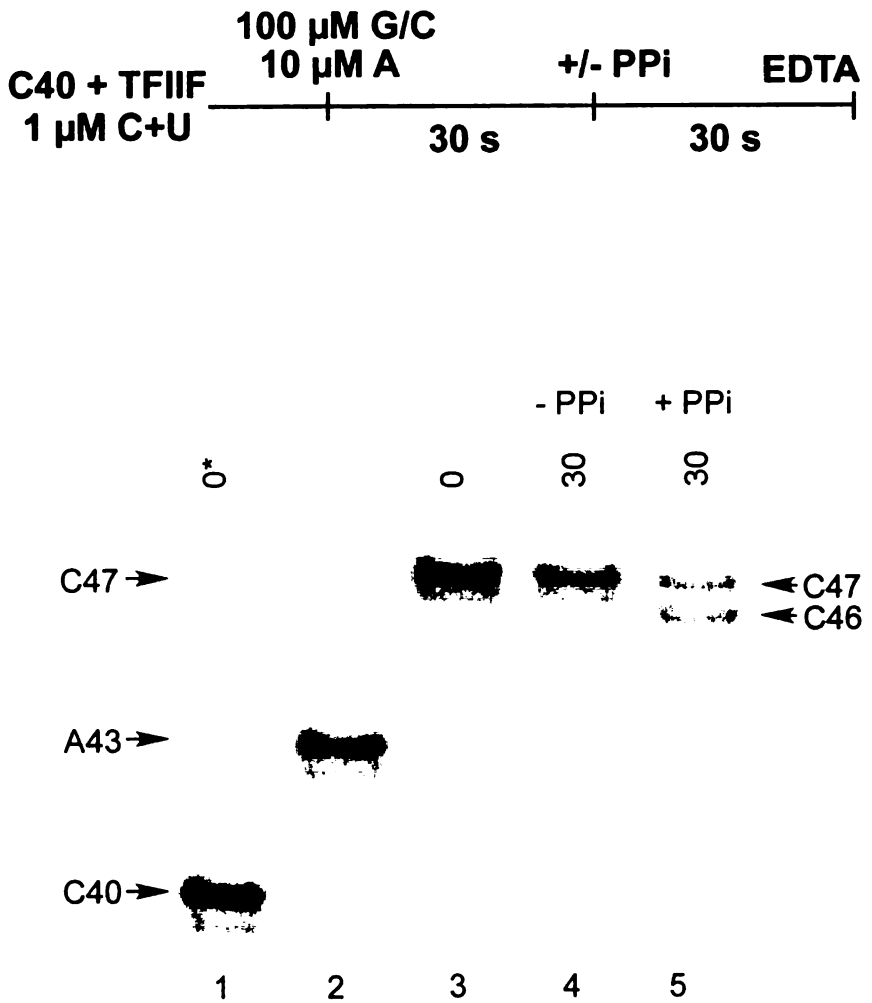

PPi was then added and incubated for 30 seconds, resulting in an approximately equal distribution of C47 and C46 complexes, confirming the dynamic equilibrium between C46 and C47 observed in Figure 2.7. We conclude that C46 results from pyrophosphorolysis from pre-translocated C47.

Experiments with PPi and NTP substrates suggest that post-translocated C46, pre-translocated C47 and post-translocated C47 complexes exist together. Because pre- and post-translocated elongation complexes co-exist at C47 in the presence of UTP substrate and PPi, this experiment provides evidence for spontaneous conversion between translocation states, even at 100 μM UTP. Such a result is consistent with translocation by sliding of the DNA duplex and RNA-DNA hybrid via a thermal ratchet at C47. This result may also be consistent with translocation through an intermediate pre-selection state (Vassylyev et al., 2007) that can be driven forward by binding NTPs and driven backward by binding PPi.

Effects of PPi and NTPs on RNAP II burst kinetics

When RNAP II is stalled by withholding the next NTP substrate, followed by substrate addition, elongation monitored by EDTA quenching follows "burst" kinetics, in which elongation complexes load and sequester the NTP-Mg^{2+} substrate very rapidly (within 0.002 seconds) (Gong et al., 2005; Nedialkov et al., 2003a; Zhang and Burton, 2004; Zhang et al., 2003). Considering PPi to be a probe for the pre-translocated elongation complex, we wished to test whether the translocation state(s) of the stalled elongation complex would be apparent. Our

expectation was that, if some fraction of stalled complexes were in the pre-translocated state, addition of 10 mM PPi would inhibit elongation. If these complexes were post-translocated, PPi should have no effect. Because NTP substrates might not be expected to bind to pre-translocated elongation complexes, PPi was expected to inhibit elongation of the pre-translocated elongation complex, however much NTP substrate was added. Phosphorimager quantification of these data (from gels shown in Figures 2.3 and 2.7) is shown in Figure 2.9.

Elongation to G44 was monitored from stalled A43 elongation complexes after adding 2.5 mM or 100 μM GTP and CTP, in the presence or absence of 10 mM PPi. At 2.5 mM GTP, "burst" kinetics of G44 synthesis was not noticeably affected by PPi, as if either: 1) no pre-translocated A43 elongation complexes contribute to the burst; or 2) GTP binds very rapidly and stably to stalled, pre-translocated A43 elongation complexes. At 2.5 mM GTP, therefore, the fraction of A43 elongation complexes that comprise the burst behave as if these complexes were post-translocated. At 100 μM GTP, however, the result is more complicated. In this case, the height of the burst is reduced by PPi addition, indicating pre-translocated A43 complexes are present. Essentially, there is competition between GTP and PPi for A43 binding. At 2.5 mM GTP, 10 mM PPi cannot compete, but at 100 μM GTP, 10 mM PPi appears to be a strong competitor for A43 binding. It is as if the A43 elongation complexes formed at the stall have characteristics of both pre- and post-translocated states depending upon the reagents that are added.

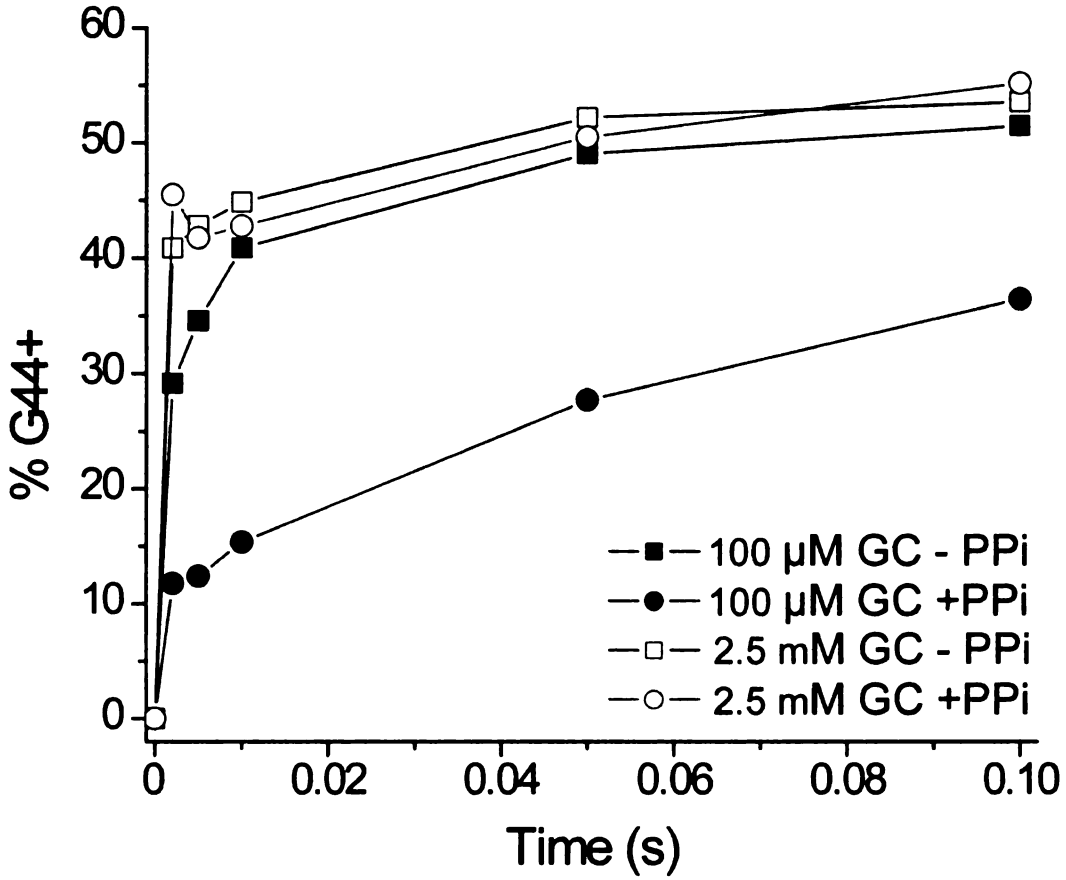

Figure 2.9 **Pyrophosphate attenuates the amplitude of the burst in G44 synthesis at 100 µM but not at 2.5 mM GTP.** Gel data (Figures 2.3 and 2.7) were quantified as % G44+ in the presence or absence of PPi.

Perhaps these elongation complexes exist in an intermediate translocation state (i.e. a pre-insertion or pre-selection site) that can be driven toward the post-translocated or pre-translocated register depending on whether GTP or PPi binds and moves the ratchet forward or in reverse.

Discussion

PPi is a by-product of RNA synthesis and can be used to drive the reverse of the polymerization reaction catalyzed by RNAP II (Chafin et al., 1995; Rozovskaya et al., 1984; Rudd et al., 1994; Sosunov et al., 2003). In this work, PPi has been assessed as a probe for the Hs RNAP II mechanism, particularly for use in transient state (pre-steady state) kinetic analyses. We find that PPi suppresses transcriptional pausing, inhibits elongation, and suppresses TFIIS-dependent dinucleotide cleavage. PPi also appears to suppress transcriptional misincorporation and has some capacity to cleave dinucleotides, apparently through endopyrophosphorolysis.

NTP-assisted translocation

PPi has been used as a probe for the pre-translocated state of the elongation complex under elongation conditions and during escape from a transcriptional stall. NTP substrates have been used as a probe for the post-translocated state of the elongation complex in competition with PPi. We find that, at high NTP concentrations (2.5 mM), inhibitory effects of PPi are overcome,

showing that 10 mM exogenous PPi addition is not sufficient to retain RNAP II in the pre-translocated state. Perhaps, NTP substrates interact with elongation complexes prior to their full forward translocation to overcome PPi inhibition. Otherwise, the observation that exogenous PPi does not noticeably inhibit elongation at high NTP concentrations is difficult to understand. Without NTP-assisted translocation at high NTP concentration, it is hard to imagine how elongation complexes can easily escape the pre-translocated state in the presence of a high concentration of exogenous PPi.

At moderate NTP concentrations (100 μM), by contrast, 10 mM PPi becomes an effective competitor of accurately templated NTP substrates, both during ongoing elongation and at a transcriptional stall. At 100 μM NTPs, there is strong evidence for Hs RNAP II cycling between the pyrophosphorolysis reaction and the forward synthesis pathway. Analysis of RNAP II "burst" kinetics during elongation from a stall position also shows NTP and PPi competition at 100 μM but not at 2.5 mM NTPs. At 10 mM PPi and 100 μM NTPs, which is close to (or above) the apparent K_d for RNAP II to bind NTPs, there is little or no evidence for NTP-assisted translocation. Physiological NTP concentrations have been estimated to be about 3.1 mM ATP, 0.47 mM GTP, 0.28 mM CTP, and 0.57 mM UTP in mammalian cells (Traut, 1994), which may be sufficient to support NTP-assisted translocation. Also, because of the prevalence of pyrophosphatases in cell nuclei, in vivo PPi levels are quite low.

Crystallographic evidence for a "pre-insertion" or "pre-selection" site for templated NTP binding may explain some of our observations. Vassylyev and

colleagues suggest that NTPs are first placed by Tt RNAP in a pre-selection site before movement into the insertion site for phosphodiester bond formation (Vassylyev et al., 2007). Transfer of the NTP into the insertion site appears to involve closing of the trigger loop-trigger helices assembly to lock the NTP substrate into the active site for chemistry, and similar closed conformations of the trigger loop-trigger helices assembly have been observed for Sc RNAP II (Vassylyev et al., 2007; Wang et al., 2006). Competition between PPi and NTPs for an intermediate translocation position appears consistent with the model that NTPs bind an intermediate translocation state (i.e. a pre-selection site) and drive it forward to a conformation that can engage in chemistry. PPi appears to suppress misincorporation by Hs RNAP II. Because PPi appears to compete with NTPs for an intermediate pre-selection site, suppression of misincorporation may result because PPi outcompetes inappropriate substrates that encounter difficulty advancing beyond the pre-selection position to the insertion site. According to this analysis, advancement from the pre-selection to the insertion position must be a determining step in transcriptional fidelity.

Thermal ratchet and NTP-assisted translocation

Hs RNAP II translocation appears to be governed by an NTP-dependent thermal ratchet. When RNAP II approaches a transcriptional stall at the C47 position, 10 mM exogenous PPi blocks completion of the previous C46 bond. This condition of apparent equilibrium between C47 synthesis (C46 post-translocated + CTP → C47 pre-translocated) and pyrophosphorolysis (C47 pre-

translocated + PPi → C46 post-translocated) is obtained at 100 μM CTP, a permissive concentration to support elongation. Because pyrophosphorolysis must launch from the pre-translocated state, and forward translocation must expose the active site for NTP binding, the C46 post-translocated state and the C47 pre-translocated state must be maintained simultaneously. When UTP substrate is added to the reaction, C46 and C47 transcripts extend to U48 and beyond. We therefore see evidence of the post-translocated C46 complex, and both the pre- and post-translocated C47 complexes, supporting the idea that multiple translocation states can exist in equilibrium. The effects of PPi and NTPs on RNAP II burst kinetics also support the idea that stalled elongation complexes can either advance to the post-translocated state or revert to the pre-translocated state depending on whether PPi or NTPs are bound. Such observations indicate a sensitively poised thermal ratchet mechanism for Hs RNAP II translocation in which PPi and NTP influence the direction in which the ratchet moves. At high templated NTP concentrations, NTP substrates overwhelm inhibitory effects of PPi, indicating that NTP-assisted forward translocation displaces the pre-translocated product complex (i.e. A43.PPi).

Suppression of pausing and TFIIS

We suggest that PPi suppresses transcriptional pausing by binding to the elongation complex and maintaining it in the pre-translocated product complex (i.e. A43.PPi). The pre-translocated product complex is an intermediate in the pyrophosphorolysis reaction and also a transient intermediate during forward

elongation in the absence of exogenous PPi. Because maintaining the product complex by addition of 10 mM exogenous PPi inhibits pausing, we suggest that RNAP II appears to enter the pausing and backtracking pathway through an intermediate that has no PPi by-product and no NTP substrate bound. Furthermore, here we show that simultaneous addition of PPi and the templated NTP substrate to a stalled RNAP II elongation complex suppresses pausing relative to addition of the templated NTP alone. This result appears to show that PPi has an active role that NTP substrates do not in releasing RNAP II from the pausing pathway.

TFIIS binds in the secondary pore of RNAP II and stimulates dinucleotide RNA cleavage (Fish and Kane, 2002; Gu and Reines, 1995; Guo and Price, 1993; Kettenberger et al., 2003; Rudd et al., 1994; Wang and Hawley, 1993). TFIIS has also been shown to cleave nascent RNA from arrested elongation complexes in larger increments than dinucleotides (Gu and Reines, 1995; Rudd et al., 1994). Therefore, TFIIS, which selectively cleaves paused elongation complexes, can be used as a probe for the pausing and backtracking pathways of RNAP II. Here, we show that exogenous PPi can inhibit TFIIS-mediated dinucleotide cleavage, apparently by maintaining the elongation complex on the active synthesis pathway and thus preventing pausing. PPi appears to stabilize the pre-translocated product complex, which is an intermediate on the active synthesis path. PPi appears to inhibit TFIIS-mediated dinucleotide cleavage by suppressing pausing. Significantly, PPi does not appear to inhibit the chemical

step of the TFIIS-mediated dinucleotide cleavage reaction but rather inhibits formation of elongation complexes that are TFIIS sensitive.

As also indicated by the work of others, PPi can participate in a dinucleotide cleavage reaction that is similar to that supported by TFIIS. This reaction appears to be endopyrophosphorolysis, as described by Luse and colleagues (Rudd et al., 1994). Because the 290-Asp-Glu-291 motif of Hs TFIIS is thought to hold a Mg^{2+} close to the tightly bound active site Mg-A of RNAP II to support dinucleotide cleavage, and because PPi is expected to chelate a Mg^{2+}, PPi is suggested to hold a Mg^{2+} in a similar position to that held by TFIIS to support an analogous dinucleotide cleavage reaction.

REFERENCES

Abbondanzieri, E.A., Greenleaf, W.J., Shaevitz, J.W., Landick, R., and Block, S.M. (2005). Direct observation of base-pair stepping by RNA polymerase. Nature *438*, 460-465.

Bar-Nahum, G., Epshtein, V., Ruckenstein, A.E., Rafikov, R., Mustaev, A., and Nudler, E. (2005). A ratchet mechanism of transcription elongation and its control. Cell *120*, 183-193.

Batada, N.N., Westover, K.D., Bushnell, D.A., Levitt, M., and Kornberg, R.D. (2004). Diffusion of nucleoside triphosphates and role of the entry site to the RNA polymerase II active center. Proc Natl Acad Sci USA *101*, 17361-17364.

Bengal, E., Flores, O., Krauskopf, A., Reinberg, D., and Aloni, Y. (1991). Role of the mammalian transcription factors IIF, IIS, and IIX during elongation by RNA polymerase II. Mol Cell Biol *11*, 1195-1206.

Chafin, D.R., Guo, H., and Price, D.H. (1995). Action of alpha-amanitin during pyrophosphorolysis and elongation by RNA polymerase II. J Biol Chem *270*, 19114-19119.

Cramer, P., Bushnell, D.A., and Kornberg, R.D. (2001). Structural basis of transcription: RNA polymerase II at 2.8 angstrom resolution. Science *292*, 1863-1876.

Fish, R.N., and Kane, C.M. (2002). Promoting elongation with transcript cleavage stimulatory factors. Biochim Biophys Acta *1577*, 287-307.

Funk, J.D., Nedialkov, Y.A., Xu, D., and Burton, Z.F. (2002). A key role for the alpha 1 helix of human RAP74 in the initiation and elongation of RNA chains. J Biol Chem *277*, 46998-47003.

Galburt, E.A., Grill, S.W., Wiedmann, A., Lubkowska, L., Choy, J., Nogales, E., Kashlev, M., and Bustamante, C. (2007). Backtracking determines the force sensitivity of RNAP II in a factor-dependent manner. Nature *446*, 820-823.

Gong, X.Q., Nedialkov, Y.A., and Burton, Z.F. (2004). Alpha-amanitin blocks translocation by human RNA polymerase II. J Biol Chem *279*, 27422-27427.

Gong, X.Q., Zhang, C., Feig, M., and Burton, Z.F. (2005). Dynamic error correction and regulation of downstream bubble opening by human RNA polymerase II. Mol Cell *18*, 461-470.

Gu, W., and Reines, D. (1995). Variation in the size of nascent RNA cleavage products as a function of transcript length and elongation competence. J Biol Chem *270*, 30441-30447.

Guo, H., and Price, D.H. (1993). Mechanism of DmS-II-mediated pause suppression by Drosophila RNA polymerase II. J Biol Chem *268*, 18762-18770.

Izban, M.G., and Luse, D.S. (1992). Factor-stimulated RNA polymerase II transcribes at physiological elongation rates on naked DNA but very poorly on chromatin templates. J Biol Chem *267*, 13647-13655.

Kahn, J.D., and Hearst, J.E. (1989). Reversibility of nucleotide incorporation by Escherichia coli RNA polymerase, and its effect on fidelity. J Mol Biol *205*, 291-314.

Kashkina, E., Anikin, M., Tahirov, T.H., Kochetkov, S.N., Vassylyev, D.G., and Temiakov, D. (2006). Elongation complexes of Thermus thermophilus RNA polymerase that possess distinct translocation conformations. Nucleic Acids Res *34*, 4036-4045.

Kettenberger, H., Armache, K.J., and Cramer, P. (2003). Architecture of the RNA polymerase II-TFIIS complex and implications for mRNA cleavage. Cell *114*, 347-357.

Kettenberger, H., Armache, K.J., and Cramer, P. (2004). Complete RNA polymerase II elongation complex structure and its interactions with NTP and TFIIS. Mol Cell *16*, 955-965.

Kireeva, M.L., Hancock, B., Cremona, G.H., Walter, W., Studitsky, V.M., and Kashlev, M. (2005). Nature of the nucleosomal barrier to RNA polymerase II. Mol Cell *18*, 97-108.

Kuhn, C.D., Geiger, S.R., Baumli, S., Gartmann, M., Gerber, J., Jennebach, S., Mielke, T., Tschochner, H., Beckmann, R., and Cramer, P. (2007). Functional architecture of RNA polymerase I. Cell *131*, 1260-1272.

Langelier, M.F., Baali, D., Trinh, V., Greenblatt, J., Archambault, J., and Coulombe, B. (2005). The highly conserved glutamic acid 791 of Rpb2 is involved in the binding of NTP and Mg(B) in the active center of human RNA polymerase II. Nucleic Acids Res *33*, 2629-2639.

Lecomte, P., Doubleday, O.P., and Radman, M. (1986). Evidence for an intermediate in DNA synthesis involving pyrophosphate exchange. A possible role in fidelity. J Mol Biol *189*, 643-652.

Lei, L., Ren, D., and Burton, Z.F. (1999). The RAP74 subunit of human transcription factor IIF has similar roles in initiation and elongation. Mol Cell Biol *19*, 8372-8382.

Lei, L., Ren, D., Finkelstein, A., and Burton, Z.F. (1998). Functions of the N- and C-terminal domains of human RAP74 in transcriptional initiation, elongation, and recycling of RNA polymerase II. Mol Cell Biol *18*, 2130-2142.

Nedialkov, Y.A., Gong, X.Q., Hovde, S.L., Yamaguchi, Y., Handa, H., Geiger, J.H., Yan, H., and Burton, Z.F. (2003a). NTP-driven translocation by human RNA polymerase II. J Biol Chem *278*, 18303-18312.

Nedialkov, Y.A., Gong, X.Q., Yamaguchi, Y., Handa, H., and Burton, Z.F. (2003b). Assay of transient state kinetics of RNA polymerase II elongation. Methods Enzymol *371*, 252-264.

Ren, D., Lei, L., and Burton, Z.F. (1999). A region within the RAP74 subunit of human transcription factor IIF is critical for initiation but dispensable for complex assembly. Mol Cell Biol *19*, 7377-7387.

Renner, D.B., Yamaguchi, Y., Wada, T., Handa, H., and Price, D.H. (2001). A highly purified RNA polymerase II elongation control system. J Biol Chem *276*, 42601-42609.

Rozovskaya, T.A., Rechinsky, V.O., Bibilashvili, R.S., Karpeisky, M., Tarusova, N.B., Khomutov, R.M., and Dixon, H.B. (1984). The mechanism of

pyrophosphorolysis of RNA by RNA polymerase. Endowment of RNA polymerase with artificial exonuclease activity. Biochem J *224*, 645-650.

Rudd, M.D., Izban, M.G., and Luse, D.S. (1994). The active site of RNA polymerase II participates in transcript cleavage within arrested ternary complexes. Proc Natl Acad Sci USA *91*, 8057-8061.

Shapiro, D.J., Sharp, P.A., Wahli, W.W., and Keller, M.J. (1988). A high-efficiency HeLa cell nuclear transcription extract. DNA *7*, 47-55.

Sosunov, V., Sosunova, E., Mustaev, A., Bass, I., Nikiforov, V., and Goldfarb, A. (2003). Unified two-metal mechanism of RNA synthesis and degradation by RNA polymerase. EMBO J *22*, 2234-2244.

Svetlov, V., Belogurov, G.A., Shabrova, E., Vassylyev, D.G., and Artsimovitch, I. (2007). Allosteric control of the RNA polymerase by the elongation factor RfaH. Nucleic Acids Res *35*, 5694-5705.

Tan, S., Aso, T., Conaway, R.C., and Conaway, J.W. (1994). Roles for both the RAP30 and RAP74 subunits of transcription factor IIF in transcription initiation and elongation by RNA polymerase II. J Biol Chem *269*, 25684-25691.

Tan, S., Conaway, R.C., and Conaway, J.W. (1995). Dissection of transcription factor TFIIF functional domains required for initiation and elongation. Proc Natl Acad Sci USA *92*, 6042-6046.

Traut, T.W. (1994). Physiological concentrations of purines and pyrimidines. Mol Cell Biochem *140*, 1-22.

Vaisman, A., Ling, H., Woodgate, R., and Yang, W. (2005). Fidelity of Dpo4: effect of metal ions, nucleotide selection and pyrophosphorolysis. EMBO J *24*, 2957-2967.

Vassylyev, D.G., and Artsimovitch, I. (2005). Tracking RNA polymerase, one step at a time. Cell *123*, 977-979.

Vassylyev, D.G., Vassylyeva, M.N., Zhang, J., Palangat, M., Artsimovitch, I., and Landick, R. (2007). Structural basis for substrate loading in bacterial RNA polymerase. Nature *448*, 163-168.

Wang, B.Q., Kostrub, C.F., Finkelstein, A., and Burton, Z.F. (1993). Production of human RAP30 and RAP74 in bacterial cells. Protein Expr Purif *4*, 207-214.

Wang, B.Q., Lei, L., and Burton, Z.F. (1994). Importance of codon preference for production of human RAP74 and reconstitution of the RAP30/74 complex. Protein Expr Purif *5*, 476-485.

Wang, D., Bushnell, D.A., Westover, K.D., Kaplan, C.D., and Kornberg, R.D. (2006). Structural basis of transcription: role of the trigger loop in substrate specificity and catalysis. Cell *127*, 941-954.

Wang, D., and Hawley, D.K. (1993). Identification of a 3'-->5' exonuclease activity associated with human RNA polymerase II. Proc Natl Acad Sci USA *90*, 843-847.

Westover, K.D., Bushnell, D.A., and Kornberg, R.D. (2004). Structural basis of transcription: nucleotide selection by rotation in the RNA polymerase II active center. Cell *119*, 481-489.

Xiong, Y., and Burton, Z.F. (2007). A Tunable Ratchet Driving Human RNA Polymerase II Translocation Adjusted by Accurately Templated Nucleoside Triphosphates Loaded at Downstream Sites and by Elongation Factors. J Biol Chem *282*, 36582-36592.

Zhang, C., and Burton, Z.F. (2004). Transcription factors IIF and IIS and nucleoside triphosphate substrates as dynamic probes of the human RNA polymerase II mechanism. J Mol Biol *342*, 1085-1099.

Zhang, C., Yan, H., and Burton, Z.F. (2003). Combinatorial control of human RNA polymerase II (RNAP II) pausing and transcript cleavage by transcription factor IIF, hepatitis delta antigen, and stimulatory factor II. J Biol Chem *278*, 50101-50111.